An Appalachian Regional Karst Map and Progress Towards a New National Karst Map

By D.J. Weary
U.S. Geological Survey, MS926A National Center, Reston, VA 20192

ABSTRACT

A new 1:1 million scale, lithology-based, digital karst map has been constructed for the Appalachian region. This map is serving as the nucleus for a new national karst map and as a test for methodologies used in developing the national karst map and data base. The map comprises data compiled from various state and regional sources. Issues encountered in the compilation process include unevenness between the various data sets in resolution, lithologic description, and classification. Regional geologic and karst data sets providing information on glacial deposits and cave and sinkhole locations are valuable components of the compilation and may also be used as tools for testing the validity of portions of the map and for creating derived products such as karst density maps. Compilation of the national karst map will become more difficult as it progresses to include semi-arid western states that contain evaporate karst, karst aquifers, karstic features propagated from buried evaporites into surface rocks of non-karstic lithology, and various features analogous to karst.

INTRODUCTION

In 2001 the U.S. Geological Survey Karst Applied Research Studies Through geologic mapping (KARST) Project began the task of constructing a new national karst map, which would improve on the Davies and others (1984) 1:7.5 million scale National Atlas karst map. The new map will be digitally-based and constructed, edited and updated in a GIS environment. The working resolution of the new map is 1:1 million scale with paper versions planned at scales of 1:7.5 and 1:2.5 million. As a first step, we are publishing a digital map of karst in the Appalachian states as a U.S. Geological Survey Open-File Report. Production of this map has revealed some of the problems and issues regarding compilation of diverse and inconsistent data sets supplied from various sources.

The Appalachian Region

The Appalachian region, as defined by the Appalachian Regional Commission (ARC) was used as an arbitrary geographic area for our initial compilation effort (fig. 1). This area, based on socio-economic and political factors, makes a compact swath covering the central and southern Appalachian Mountains, the Piedmont and parts of the eastern Midcontinent, Atlantic Coastal Plain, and the Gulf Coastal Plain. This area includes the states of New York, Pennsylvania, Ohio, Maryland, Virginia, West Virginia, Kentucky, North Carolina, Tennessee, South Carolina, Georgia, Alabama, and Mississippi. Included on our map, so that it will be complete to the Atlantic coast, are the states of New Jersey and Delaware.

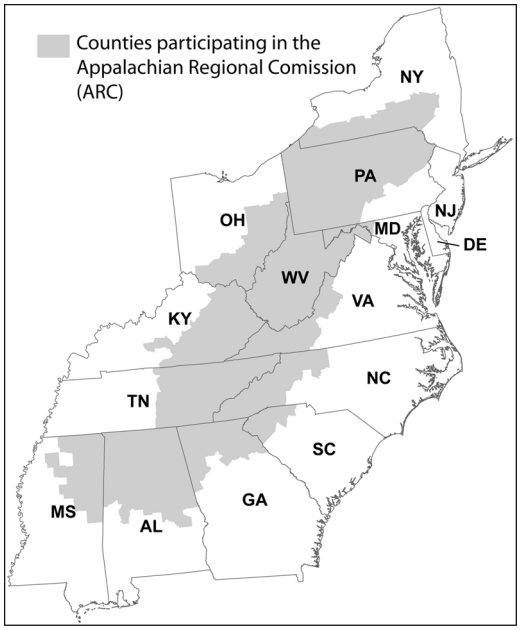

Figure 1. The Appalachian region as defined by the ARC, in gray. States of New Jersey and Delaware are included in this study for completeness to the Atlantic coast.

COMPILATION

Karst and Geologic data

Representatives of all of the state geological surveys in the region were contacted and invited to participate in a workshop on Appalachian karst sponsored by the U.S. Geological Survey and the Kentucky Geological Survey in September, 2002. States that could not attend were asked for sources of karst or geologic data or publicly available geologic data were located on the internet. Karst or geologic data at a scale of 1:1 million or larger were acquired for each state and loaded into ArcMap-ArcInfo for manipulation.

Some states, such as Kentucky and Ohio, already had a state-scale karst map completed (Appendix 1). Those karst areas were simply incorporated into the map and assigned the appropriate attributes. For other areas it is assumed that, in the eastern U.S., where there is sufficient rainfall, carbonate areas, extracted from bedrock maps would suffice as proxies for areas of karst. Geologic units with no carbonates in their unit description were deleted. Lithologic unit descriptions from the original data sets were cross-checked against descriptions in the U.S. Geological Survey National Geologic Map Database (http://ngmdb.usgs.gov/Geolex/geolex_home.html). References to data sources for each state are listed in Appendix 1.

Since the resolution of the individual data sources varied from scales of 1:1 million to 1:24,000 the distance between vertices in the polygon boundaries was generalized in ArcInfo to a spacing of 150 meters for uniformity and to eliminate some of the very small polygons and curves that would not be visible at the working scale of 1:1 million. Also, all polygons with an area of less than 40,000 m^2 were deleted, as they are too small to portray visibly on the map.

Each polygon was then assigned the following attributes: 1). K_TYPE = an abbreviation for the karst type; state = state name; REF_CODE = reference code, an alphanumeric code to the data source(s).

Structural data

After the areal distribution of potentially karstic rocks was mapped, a scanned and georegistered image of a Tectonic lithofacies map of the Appalachian orogen (Williams, 1978) was used as a visual template for segregating folded and faulted rocks east of the Allegheny structural front from flat-lying to gently dipping rocks to the west. The rationale for this division is the strong influence that the structural nature of the host bedrock has on cave passage patterns and, presumably, other karst features (Palmer, 2000).

Glacial data

Because glacial beveling and cover by glacial sediments has a profound effect on karst distribution in the northern portion of the United States, data on thickness of glacial sediments were integrated into the karst map. Fortunately, a digital dataset of glacial sediment cover for the United States east of the Rocky Mountains already exists (Soller and Packard, 1998). Areas with glacial cover exceeding 50 ft thick (fig. 2) were extracted from this dataset and intersected with the karst areas to define areas of potential karst buried under glacially derived sediments.

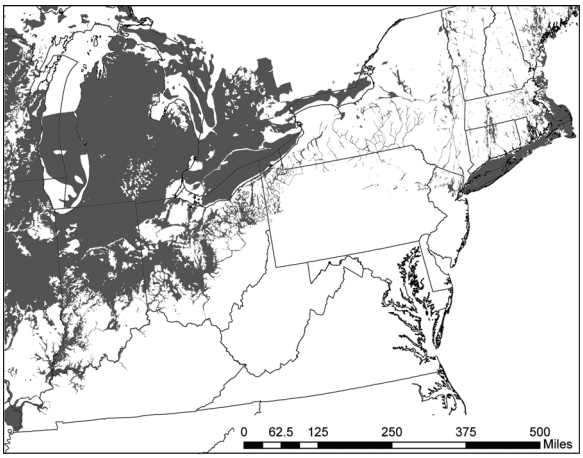

Figure 2. Distribution of glacial sediments greater than 50 ft thick (in gray) in part of the Appalachian region. Derived from data from Soller and Packard (1998).

RESULTS

A draft, first version of the Appalachian karst map is shown in figure 3. A portion of the Davies

TJB- Triassic and Jurassic basin fill calcareous sediments. Includes calcareous conglomerates and minor lacustrine limestones. Dissolution may result in solution and subsidence sinkholes and small caves.

DISCUSSION

Problems

Most of the major problems in the new map are differences in delineation of karst areas across state boundaries on state geologic maps. Karst areas for the state of Pennsylvania and the edges of the adjoining states are shown on figure 5 to illustrate some of these differences. Notice that areas delineated as karstic in western Pennsylvania are not currently identified in Ohio and West Virginia. These areas were, however, shown in a gross manner in the Davies and others (1984) (fig. 4) map.

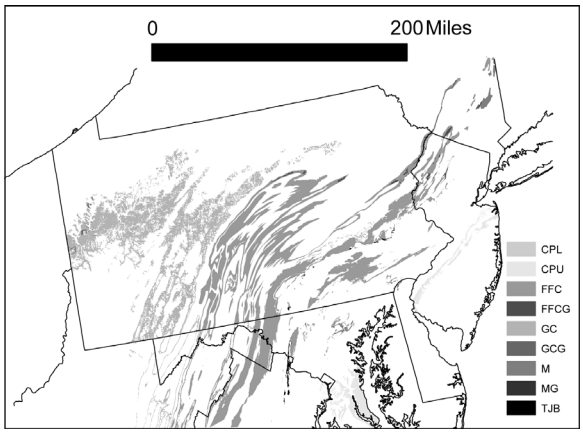

Figure 5. The Pennsylvania portion of the new Appalachian karst map showing discontinuities across boundaries of neighboring states. Explanation of map units as in figure 3.

These areas represent the extent of the Pennsylvanian Allegheny Formation and the Mississippian Mauch Chunk Formation (Miles and others, 2001). The Allegheny Formation comprises chiefly clastic rocks, but also contains the Vanport Limestone which contains caves and other karst features. Likewise, the Mauch Chunk Formation includes the Loyalhanna, Greenbrier, Wymps Gap, and Deer Valley Limestones. The Loyalhanna and Greenbrier Limestones, in particular, contain caves and other karst features. The Vanport was probably not included in the state karst map of Ohio (Pavey and others, 2002) because it thins to less than 10 ft thick west of the Ohio River.

Some belts of carbonate units equivalent-in-part to the Mississippian Mauch Chunk Formation-continue on into Maryland and West Virginia but are thinner and discontinuous having been subdivided from the thicker clastic units in those states (Peper and others, 2001; West Virginia Bureau of Public Health, 1998).

Ongoing work to compile and refine karst maps of Pennsylvania by Bill Kochanov at the Pennsylvania Geological Survey (oral commun., 2005) will be incorporated in the Appalachian map in the future to revise the extent of karst within that state and will probably resolve most of the boundary mismatches with Maryland and West Virginia. In addition the extent of the Vanport Limestone will probably be extended to the west, feathering-out in eastern Ohio.

A section of the Appalachian karst map centered on the Atlantic Coastal Plain areas of North and South Carolina is shown on Fig. 6. The medium and dark gray areas delineate potentially karstic units derived from individual state data sources. There is not good matching between the mapped Coastal Plain units across the state borders. Differences in lithologic descriptions and each state's classification and grouping scheme affect the aerial extent of the units. Some areas of potential karst, especially in the unconsolidated units, are undoubtedly overstated. Areas of light gray on figure 6 show the extent of potentially karstic units derived from a database for the entire Atlantic Coastal Plain (Newell and others, unpublished data) and areas of very dark gray indicates the overlap of that data set with kart areas delineated by the individual state data. Use of the regional data set eliminates most of the discontinuities between the state boundaries, but, because it is focused on surficial units it does not include some important bedrock limestone units such as the Eocene Castle Hayne Limestone in eastern North Carolina.

Resolution of these problems in the Coastal Plain will require combining the information from the various data sets and a search for more detailed

information on the distribution of calcareous sediments and whether there are, in fact, karst features in some of these units.

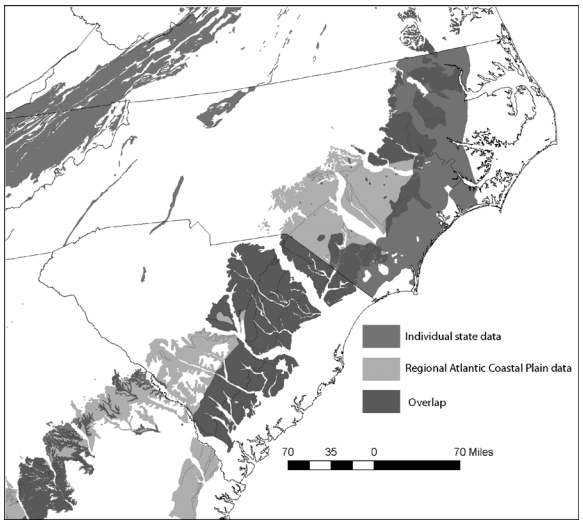

Figure 6. The North and South Carolina part of the new Applachian Karst map showing discontinuities in data sets.

Reported cave locations in the U.S., east of the Mississippi River, plotted on the Appalachian karst map are shown on figure 7. Because they cross state lines and are, presumably, evenly sampled, regional data sets such as this are valuable for checking the accuracy of the karst delineation. Data sets for other karst features, such as sinkhole and spring locations also exist, although most are limited to a particular state or smaller area. If some of these data can be acquired and joined together they will enable further geostatistical analyses of karst across large areas. The density of caves within a part of the Appalachian karst map is shown in figure 8 as an example. This particular plot was generated purely for demonstration purposes, with little thought to rigorous statistical meaning, and should not be taken seriously at this point. It does, however, show interesting patterns in the variation of cave density, with concentrations of caves in central Kentucky, the northeastern corner of Alabama and the southwestern tip of Virginia. Future studies of regional karst feature distribution should lead to new ideas about the effect of tectonism, lithologic facies, hydrologic regime, glaciation, and other factors on the intensity of karstification.

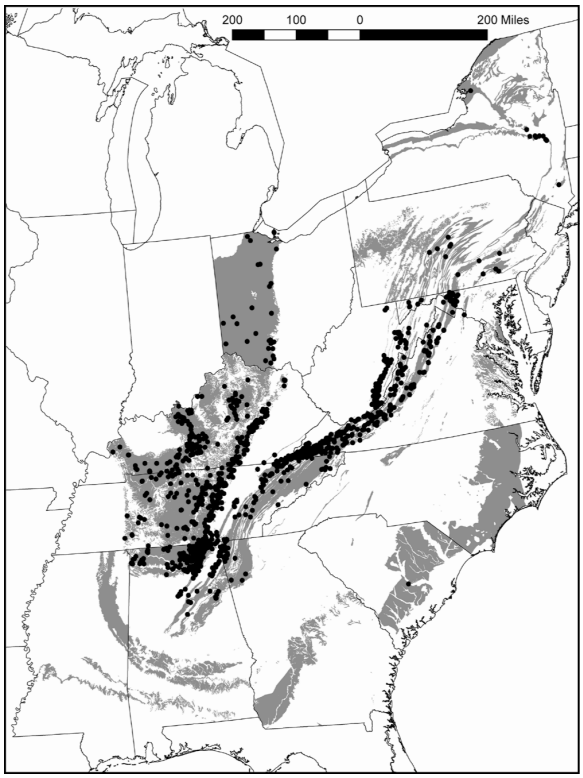

Figure 7. Cave locations (black dots, n=1395) plotted on karst areas in the Appalachians. Cave location data from David Culver, American University, 2004, written communication.

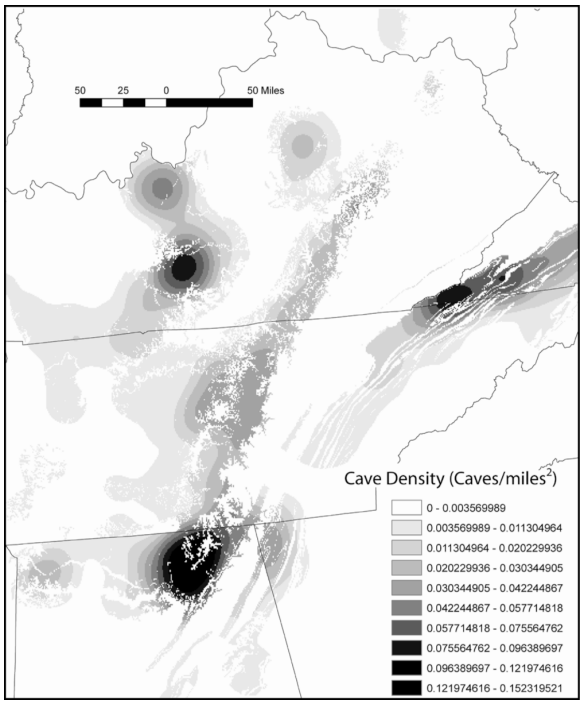

Figure 8. Cave density mapped within the Appalachian karst polygons.

As the nucleus formed by the Appalachian karst map is solidified, state by state coverages, forming the new National Karst map, will be accreted to it. Classifying karst areas in the western part of the country will be a challenge. West of the 32.5-in. mean precipitation line, the nature of wearthering and expression of karst features in the United States changes (fig. 9; Epstein and Johnson, 2003). Issues include mapping buried karst, deeply buried evaporates that propagate karst features to non-karstic rocks at the surface, and where to cut the continuum from surface karstic rocks into karst aquifers. A U.S. Geological Survey sponsored workshop involving the state geological surveys of Kansas, Arkansas, Illinois, Iowa, Nebraska, and Wisconsin focusing on these issues will be held August 17 and 18, 2005 at the Kansas Geological Survey. Hopefully we can make some real progress towards generating rules of thumb for mapping these phenomena.

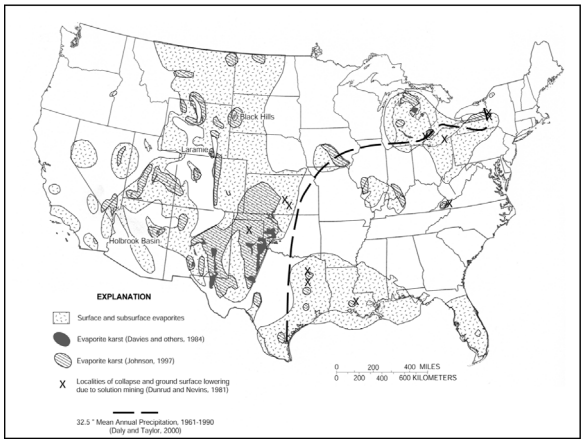

Figure 9. Map showing distribution of outcropping and subsurface evaporate rocks in the United States and areas of reported evaporate karst. The 32.5-in. mean-annual-precipitation line approximates the boundary between eastern and western karst (from Epstein and Johnson, 2003, fig. 5)

REFERENCES

Daly, C., and Taylor, G., 2000, United States average annual precipitation, 1961-1990: Spatial Climate Analysis Service, Oregon State University; USDA-NRCS National Cartography and Geospatial Center, Fort Worth, Texas; online linkage: http://www.ftw.nrcs.usda.gov/prismdata.html.

Davies, W.E., Simpson, J.H., Ohlmacher, G.C., Kirk, W.S., and Newton, E.G., 1984, Engineering aspects of karst: U.S. Geological Survey, National Atlas, scale 1:7,5000.

Dunrud, C.R., and Nevins, B.B., 1981, Solution mining and subsidence in evaporate rocks in the United States: U.S. Geological Survey Miscellaneous Investigation Series Map I-1298, 2 sheets.

Epstein, J.B., and Johnson, K.S., 2003, The need for a national evaporate karst map, in Johnson, K.S. and Neal, J.T., eds., Evaporite karst and engineering/environmental problems in the United States: Norman, Oklahoma Geological Survey, Circular 109, p. 21-30.

Johnson, K.S., 1997, Evaporite karst in the United States: Carbonates and Evaporites, v. 12, p. 2-14.

Miles, C.E., Whitfield, G.T. and other staff and interns of the Pennsylvania Geological Survey, 2001, Bedrock geologic units of Pennsylvania, based on: Berg, T.M., Edmunds, W.E., Geyer, A.R., Glover, A.D., Hoskins, D.M., MacLachlan, D.B., Root, S.I., Sevon, W.D., and Socolow, A.A., 1980, Geologic map of Pennsylvania: Pennsylvania Geological Survey, Map 1, scale 1:250000. http://www.dcnr.state.pa.us/topogeo/map1/bedmap.aspx

Palmer, A.N., 2000, Hydrogeologic control of cave patterns, *in* Klimchouk, A.B. and others, eds., Spelogenesis evolution of karst aquifers: Huntsville, National Speleological Society, p. 77-90.

Pavey, R.R., Hull, D. N., Brockman, C. S., Schumacher, G. A., Stith, D. A., Swinford, E. M., Sole, T.L., Vorbau, K. E., Kallini, K. D., Evans, E. E., Slucher, E. R., and R. G. Van Horn, 2002, Known and probably karst in Ohio, 2002: Ohio Geological Survey, EG-1, version, GIS data on CD provided by the Ohio Geological Survey, scale 1:24,000.

Peper, J.D., McCartan, L.B., Horton, J.W., Jr., and Reddy, J.E., 2001, Preliminary lithogeochemical map showing near-surface rock types in the Chesapeake Bay watershed, Virginia and Maryland: U.S. Geological Survey Open-File Report 01-187, resolution 1:500,000.Maryland part based on the Cleaves, 1968, Geologic map of Maryland. http://pubs.usgs.gov/open-file/of01-187/

Soller, D.R. & Packard, P.H. (1998). Digital representation of a map showing the thickness and character of Quaternary sediment in the glaciated United States east of the Rocky Mountains: U.S. Geological Survey

Digital Data Series DDS-38, scale 1:1,000,000. http://pubs.usgs.gov/dds/dds38/shape.html

Tobin B.D. and Weary, D.J., 2004, Digital Engineering Aspects of Karst Map: A GIS Version of Davies, W.E., Simpson, J.H., Ohlmacher, G.C., Kirk, W.S., and Newton, E.G., 1984, Engineering Aspects of Karst: U.S. Geological Survey, National Atlas of the United States of America, Scale 1:7,500,000. http://pubs.usgs.gov/of/2004/1352/

West Virginia Bureau of Public Health, 1998, Karst regions derived from 1968 geological map of West Virginia: West Virginia GIS Technical Center, online data http://wvgis.wvu.edu/data/dataset.php?action=search&ID=133, resolution 1:250,000.

Williams, Harold, compiler,1978, Tectonic lithofacies map of the Appalachian orogen: St John's : Memorial University of Newfoundland, scale 1:1 000,000.

APPENDIX 1

State by state annotated sources for karst and geologic data (in alphabetical order)

Alabama - Szabo, M.W., Osborne, W.E., Copeland, C.W., Jr., and Neathery, T.L., 1988, Geologic Map of Alabama: Geological Survey of Alabama, Special Map 200; digital version: Digital geologic map of Alabama, Beta Version 1, 2002: Geologic Survey of Alabama, scale 1:250,000. [Used for entire state]

Delaware - Nenad Spoljaric, Jordan, R.R., Generalized geologic map of Delaware, revised 1976 by Pickett, T.E.: Delaware Geological Survey, 1 sheet, scale ca. 1:600,000. [Map scanned and digitized at U.S. Geological Survey; Used for entire state]

Georgia - Alhadeff, J.S., Musser, J. W., Sandercock, A.C., and Dyar, T.R., 2001, Digital environmental atlas of Georgia: Georgia Geologic Survey Publication CD-1, ver. 2., scale 1:250,000. [Used for entire state]

Kentucky –Paylor, R.L., and Currens, J.C., 2002, Karst Occurrence in Kentucky: Kentucky Geological Survey, KGS Map and Chart 33, scale 1:500,000. http://www.uky.edu/KGS/water/general/karst/karst-gis.htm . [Used for entire state].

Maryland - Peper, J.D., McCartan, L.B., Horton, J.W., Jr., and Reddy, J.E., 2001, Preliminary lithogeochemical map showing near-surface rock types in the Chesapeake Bay watershed, Virginia and Maryland: U.S. Geological Survey Open-File Report 01-187, resolution 1:500,000.Maryland part based on the Cleaves, 1968, Geologic map of Maryland. http://pubs.usgs.gov/openfile/of01-187/ [Used for entire state, except Coastal Plain]

Newell, W. L, Prowell, D., Kranz, D., Powars, D., Mixon, R., Weems, R., Stone, B., and Willard, D., Surficial geology and geomorphology of the Atlantic Coastal Plain: U.S. Geological Survey, unpublished data.; [Used in Coastal Plain only]

Mississippi - Online data from Mississippi Automated Resource Information System (MARIS) at: http://www.maris.state.ms.us/HTM/Data%20Warehouse/Statewide_alpha.htm. No metadata available (4/2004) scale 1:500,000. [Map units compared with descriptions on published paper maps: 1. Bicker, A.R. Jr., (compiler) 1985, Geologic Map of Mississippi: Mississippi Geological Survey, scale 1:500,000. 2. Booth, D.C. and Schmitz, D.W. (compilers), 1983, Economic minerals map of Mississippi: Mississippi Bureau of Geology, Mississippi Mineral Resources Insititute, scale 1:500,000.]

New Jersey - Vector graphic files of karst units of New Jersey were supplied by Donald Monteverde, New Jersey Geological Survey and were converted to GIS at the U.S. Geological Survey. These units were extracted from: 1.) Dalton, R.F., 1996, Bedrock geologic map of northern New Jersey: U.S. Geological Survey, Miscellaneous Investigations Series, I-2540-A, scale 1:100,000. 2.) Owens, J.P., Sugarman, P.J., Sohl, N.F., Parker, R.A., Houghton, H.F., Volkert, R.A., Drake, A.A., and Orndorff, R.C., 1995, Geologic map of New Jersey: central sheet: New Jersey Geological Survey, scale 1:100,000. 3.) Owens, J.P., Sugarman, P.J., Sohl, N.F., Parker, R.A., Houghton, H.F., Volkert, R.A., Drake, A.A., and Orndorff, R.C., 1995, Geologic map of New Jersey: southern sheet: New Jersey Geological Survey, scale 1:100,000. [Used for entire state.]

New York - Fickies, R.H. and Fallis, E., 1996, Rock Type Map of New York State: New York State Geological Survey, Open file Report 1g1222, scale 1:1,000,000. [GIS data provided by the New York Geological Survey; Used for entire state.]

North Carolina - North Carolina Geological Survey, 1999, Geology - North Carolina: North Carolina Department of Environment and Natural Resources -Division of Land Resources, North Carolina Corporate Geographic Database online data, http://www.geology.enr.state.nc.us/gis/geol250d.htm. resolution 1:250,000. [Calcareous rocks extracted based on description of map units. Used for entire state.]

Ohio - Pavey, R.R., Hull, D. N., Brockman, C. S., Schumacher, G. A., Stith, D. A., Swinford, E. M., Sole, T.L., Vorbau, K. E., Kallini, K. D., Evans, E. E., Slucher, E. R., and R. G. Van Horn, 2002, Known and probable karst in Ohio, 2002: Ohio Geological Survey, EG-1, version, GIS data on CD provided by the Ohio Geological Survey, scale 1:24,000. [Polygons generalized and reclassified. Used for entire state.]

Pennsylvania - Miles, C.E., Whitfield, G.T. and other staff and interns of the Pennsylvania Geological Survey, 2001, Bedrock geologic units of Pennsylvania, based on: Berg, T.M., Edmunds, W.E., Geyer, A.R., Glover, A.D., Hoskins, D.M., MacLachlan, D.B., Root, S.I., Sevon, W.D., and Socolow, A.A., 1980, Geologic map of Pennsylvania: Pennsylvania Geological Survey, Map 1, scale 1:250000. http://www.dcnr.state.pa.us/topogeo/map1/bedmap.aspx [Carbonate units extracted based on map descriptions. Used for Entire state.]

South Carolina - Horton, J.W. Jr., 2001, Preliminary digital geologic map of the Appalachian Piedmont and Blue Ridge, South Carolina Segment: U.S. Geological Survey, Open-file Report 01-298, http://pubs.usgs.gov/openfile/of01-298/, scale 1:500,000. [Carbonate units extracted based on unit labels and descriptions of units found in the U.S. Geological Survey Geologic names lexicon: http://ngmsvr.wr.usgs.gov/Geolex/geolex_home.html; Used for Blue Ridge and Piedmont Provinces only.]

Newell, W. L, Prowell, D., Kranz, D., Powars, D., Mixon, R., Weems, R., Stone, B., and Willard, D., Surficial geology and geomorphology of the Atlantic Coastal Plain: U.S. Geological Survey, unpublished data: [Carbonate units extracted based on unit labels and descriptions of units found in the U.S. Geological Survey Geologic names lexicon: http://ngmsvr.wr.usgs.gov/Geolex/geolex_home.html; Used for Coastal Plain province only.]

Tennessee - Greene, D.C., and Wolfe, W.J., 2000, Superfund GIS – 1:250,000 geology of Tennessee: U.S. Geological Survey, digital version of Tennessee Division of Geology, 1966, Geologic map of Tennessee: Tennessee Division of Geology, William D. Hardeman, State Geologist, 4 sheets, scale 1:250,000. http://water.usgs.gov/GIS/metadata/usgswrd/geo250k.html [Calcareous rocks extracted based on description of map units. Used for entire state.]

Virginia - Virginia Division of Mineral Resources, 2003, Digital representation of the 1993 geologic map of Virginia: Virginia Division of Mineral Resources Publication 174 [CD-ROM; 2003, December 31]. Adapted from Virginia Division of Mineral Resources, 1993, Geologic map of Virginia and Expanded Explanation: Virginia Division of Mineral Resources, scale 1:500,000. [Calcareous rocks extracted based on description of map units. Used for entire state.]

West Virginia - West Virginia Bureau of Public Health, 1998, Karst regions derived from 1968 geological map of West Virginia: West Virginia GIS Technical Center, online data http://wvgis.wvu.edu/data/dataset.php?action=search&ID=133, resolution 1:250,000. [Used for entire state.]

Hydrogeologic-Framework Mapping of Shallow, Conduit-Dominated Karst—Components of a Regional GIS-Based Approach

By Charles J. Taylor [1], Hugh L. Nelson Jr. [1], Gregg Hileman [2], and William P. Kaiser [3]
[1]USGS Kentucky Water Science Center, Louisville, KY
[2]USGS Tennessee Water Science Center, Nashville, TN
[3]USGS HQ Geographic Information Office, Sacramento, CA

INTRODUCTION

Recent advancements in geographic information system (GIS) technology, coupled with the increased availability of Internet-accessible geospatial datasets such as Digital Elevation Models (DEMs), Digital Orthophoto Quadrangles (DOQs), and Digital Raster Graphic Maps (DRGs), have greatly improved the compilation, interpretation, and visualization of information needed to address water-resources management and protection issues. As applied to karst hydrogeologic studies, GIS is an exceptionally useful way to assemble and process the complex datasets needed to map karst hydrogeologic features (Florea and others, 2002; Gao, 2002) and also provides an effective means of identifying important but sometimes obscure relations between surface and subsurface components of karst aquifer systems (Veni, 1999, 2003).

This Abstract briefly describes the GIS-based approach being applied to synthesize available hydrogeologic mapping data as part of a regional karst study being conducted by the U.S. Geological Survey (USGS) Ground-Water Resources Program. The focus of the regional study is the shallow, conduit-dominated karst aquifers of the Interior Low Plateaus physiographic region of the United States (fig. 1). These aquifers are located in seven geographically distinctive karst terranes (fig. 1) that exhibit similar hydrogeologic characteristics. The framework for the karst aquifers in each of the seven terranes consists of contiguous karst drainage basins. Each karst drainage basin is defined by a specific geographic area where surface and ground water are highly interconnected and contribute to the flow within a dentritic conduit drainage network (fig. 2). Typically, each karst drainage basin discharges to a large perennial karst spring that functions as the primary drainage element of a high-flow distributary (Quinlan and Ewers, 1989). The hydrologic behavior of the karst drainage basins and the springs is greatly affected, and often dominated, by concentrated recharge that originates as stormwater runoff drained rapidly to the subsurface by way of sinkholes and sinking streams. However, the bulk of the annual recharge to the karst drainage basins occurs by dispersed infiltration of precipitation through the soil and by water stored and released from a leaky epikarst zone (Ray, 2001).

COMPONENTS OF THE GIS-BASED APPROACH

Much of the first year of the study has been devoted to gathering available data and to developing GIS methods and datasets needed to map major karst hydrogeologic features at local to regional scale. Components of the GIS-based mapping approach include (1) sinkhole locations and catchment areas defined by processing of DEMs, (2) springs identified in the USGS National Water Information System (NWIS) database, (3) topographic drainage divides derived from DEMs, (4) identified sinking or losing streams and relic stream valleys (karst paleovalleys), (5) other hydrographic features such as perennial “blue line” streams and ponds or lakes, (6) 8- and 10-digit hydrologic unit (HU) boundaries, (7) vectors representing subsurface flow paths inferred from reported dye-tracer test results, and (8) boundaries of karst drainage basins inferred by dye-tracer tests and other hydrogeologic-mapping techniques.

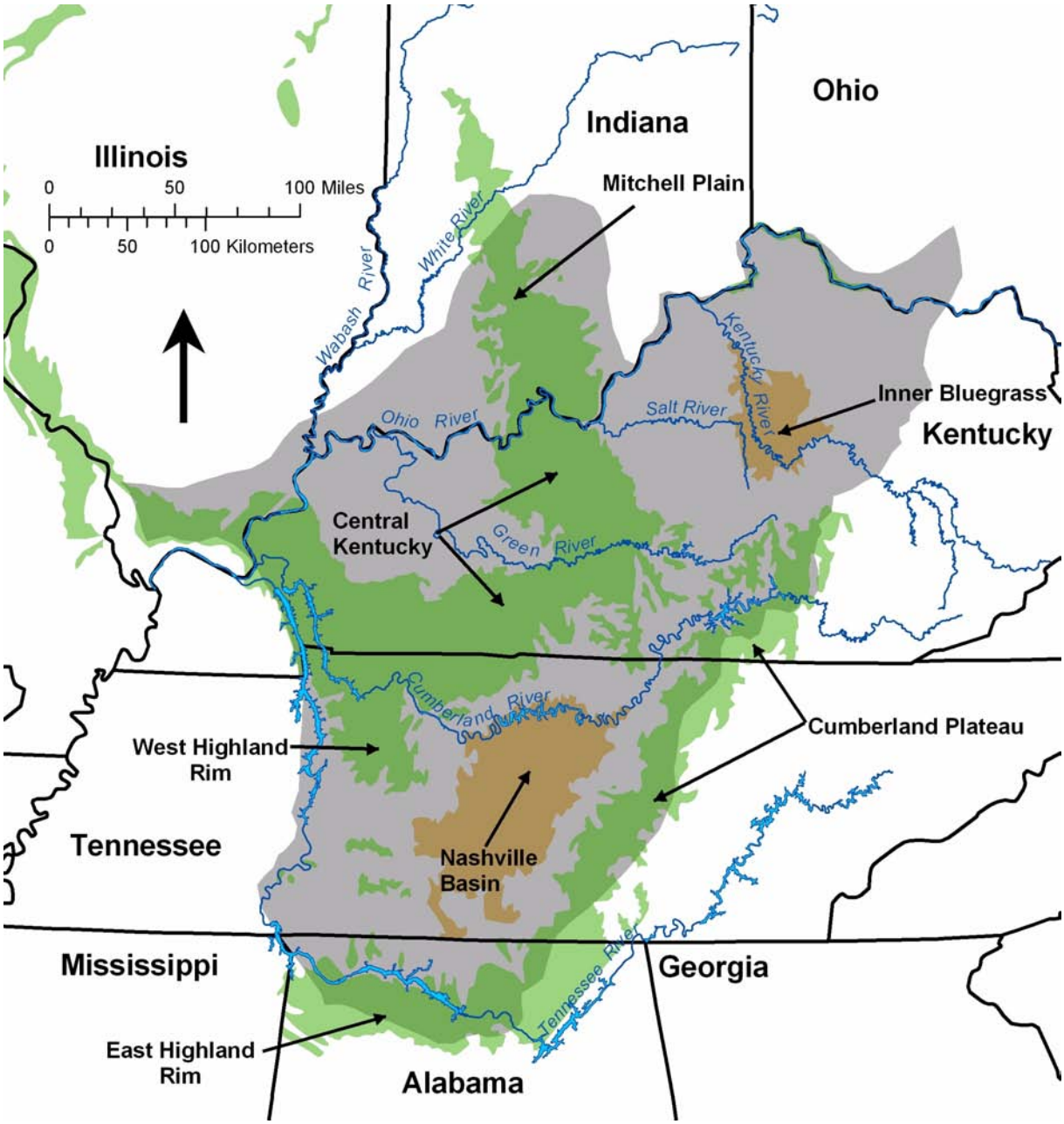

Figure 1. Interior Low Plateaus regional study area and its seven major karst terranes: (1) Mitchell Plain; (2) Central Kentucky; (3) Inner Bluegrass; (4) West Highland Rim; (5) Nashville Basin; (6) Cumberland Plateau; and (7) East Highland Rim.

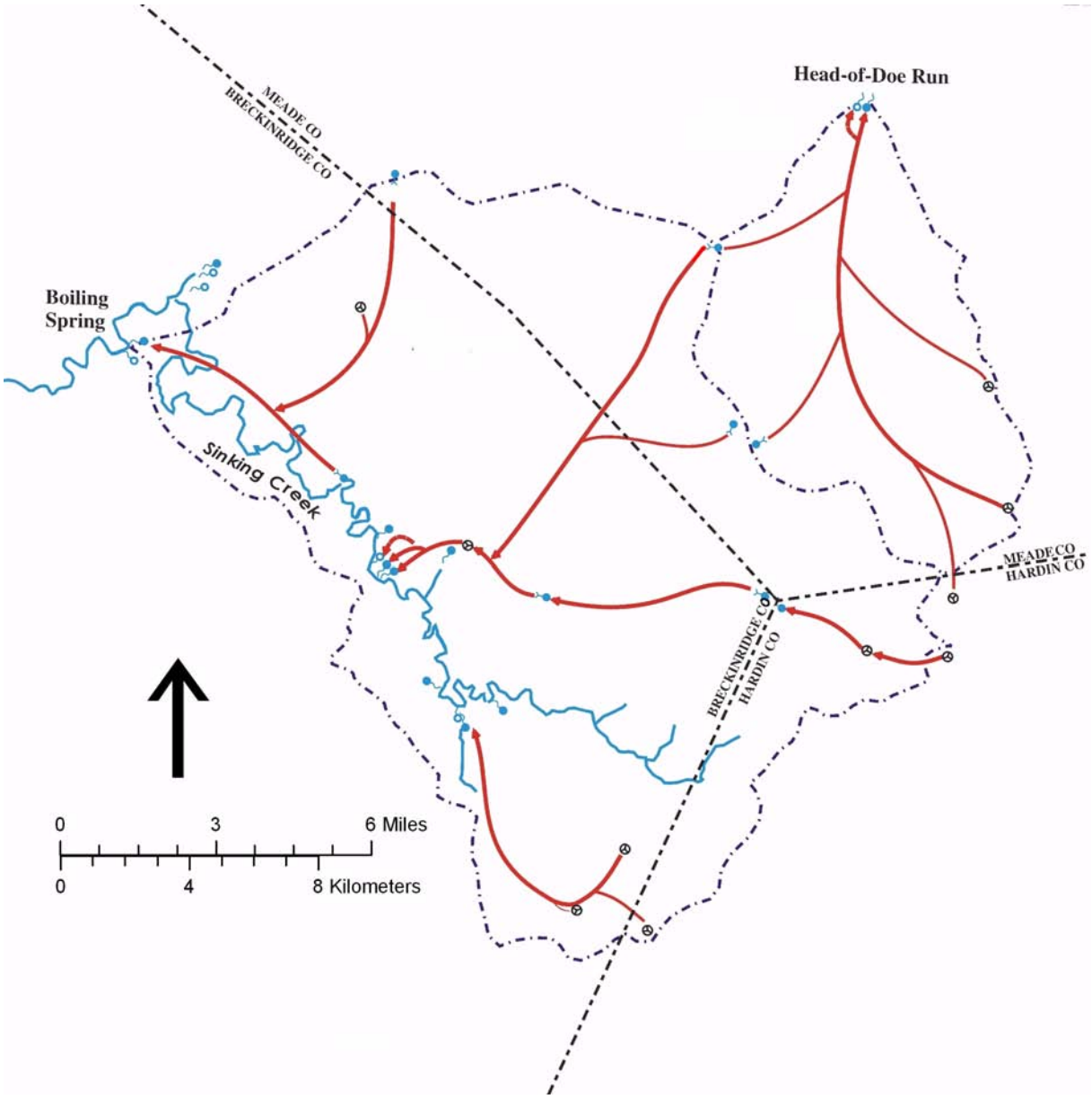

Figure 2. Dendritic conduit flow paths, inferred by dye-tracer test results (curvilinear arrows), are typical of karst drainage basins in the regional study area. This example illustrates the flow paths and basin boundaries (dashed lines) delineated for Boiling Spring and Head-of-Doe Run Spring in the Central Kentucky karst terrane. (Modified from Joe Ray, Kentucky Division of Water, unpub. data, 2005).

Of the eight components listed above, dye-tracer test data are the most crucial and difficult to obtain. A considerable effort has been made to identify sources of, and obtain, all available (i.e., publicly accessible) dye-tracer test data in the region. However, with the exception of Kentucky, where a systematic effort is being made by State agencies to map karst flow paths and drainage basin boundaries (Currens and Ray, 1999), the availability and quality of dye-tracer test data vary greatly. In general, dye-tracer test data are clustered in certain geographic areas within each of the seven karst terranes delineated in figure 1. Where dye-tracer test data are too sparse or lacking, GIS mapping of subsurface flow paths and karst drainage basin boundaries is not possible. Nevertheless, in these areas, as elsewhere in the region, the surficial karst features are being mapped, analyzed, and compared.

One goal of this work is to obtain a regional karst features database—composed of the eight hydrogeologic mapping components listed above—assembled as print-publishable map files (PMFs) that can be viewed and manipulated using ArcMap[1] or ArcReader GIS software. To emphasize the direct interconnection between ground and surface water in karst terranes, a watershed cataloguing scheme is being used to index the PMFs: first, by 8-digit HU codes; second, by 10-digit HU codes. An example of the watershed cataloguing scheme is shown in figure 3, which presents DEM data processed with GIS to delineate the 10-digit HUs, or topographic subbasins, included in the 8-digit Upper Green River HU (watershed) in the Central Kentucky karst terrane. This cataloguing scheme will facilitate evaluation and comparison of karst features within and among regional surface watersheds and will aid the transfer of karst hydrologic data to the USGS National Hydrography Dataset (NHD) (http://nhd.usgs.gov/) and The National Map project (http://nationalmap.gov/).

The synthesis of data by watersheds also provides a useful means to easily correct or refine HU boundaries, which are used as basic water-accounting units by the NHD and are needed for a variety of Federal and State environmental and water-use regulatory programs. If HU boundaries, which are mapped using topographic drainage divides, are not corrected in karst areas to account for subsurface conduit routing of flow into or out of surface watersheds, appreciable errors may be introduced to the delineation of the contributing areas of surface streams, karst aquifer boundaries, and hydrologic calculations or models (Currens and Ray, 1999). Examples of this potential problem are shown in figure 3, where the inserts (figs. 3A and 3B) illustrate two locations in the Upper Green River watershed that the boundaries mapped for constituent 10-digit HUs do not coincide with the boundaries of the actual contributing area as determined by dye-tracing tests. The errors potentially introduced by assigning and using HU boundaries without correcting for karst drainage can be appreciable. In this case, approximately 75 percent of the Upper Green River's drainage area is misattributed to the Barren River—an adjacent 10-digit HU (Ray, 2001). In a preliminary assessment, using available dye-tracer test data, Ray and others (2000) estimated that approximately 15 to 20 percent of the Central Kentucky karst terrane may exhibit such "misbehaved" drainage. The extent of this potential problem in the other karst terranes in the regional study area has not been determined.

[1]Any use of trade, product, or firm names in this publication is for descriptive purposes only and does not imply endorsement by the U.S. Government.

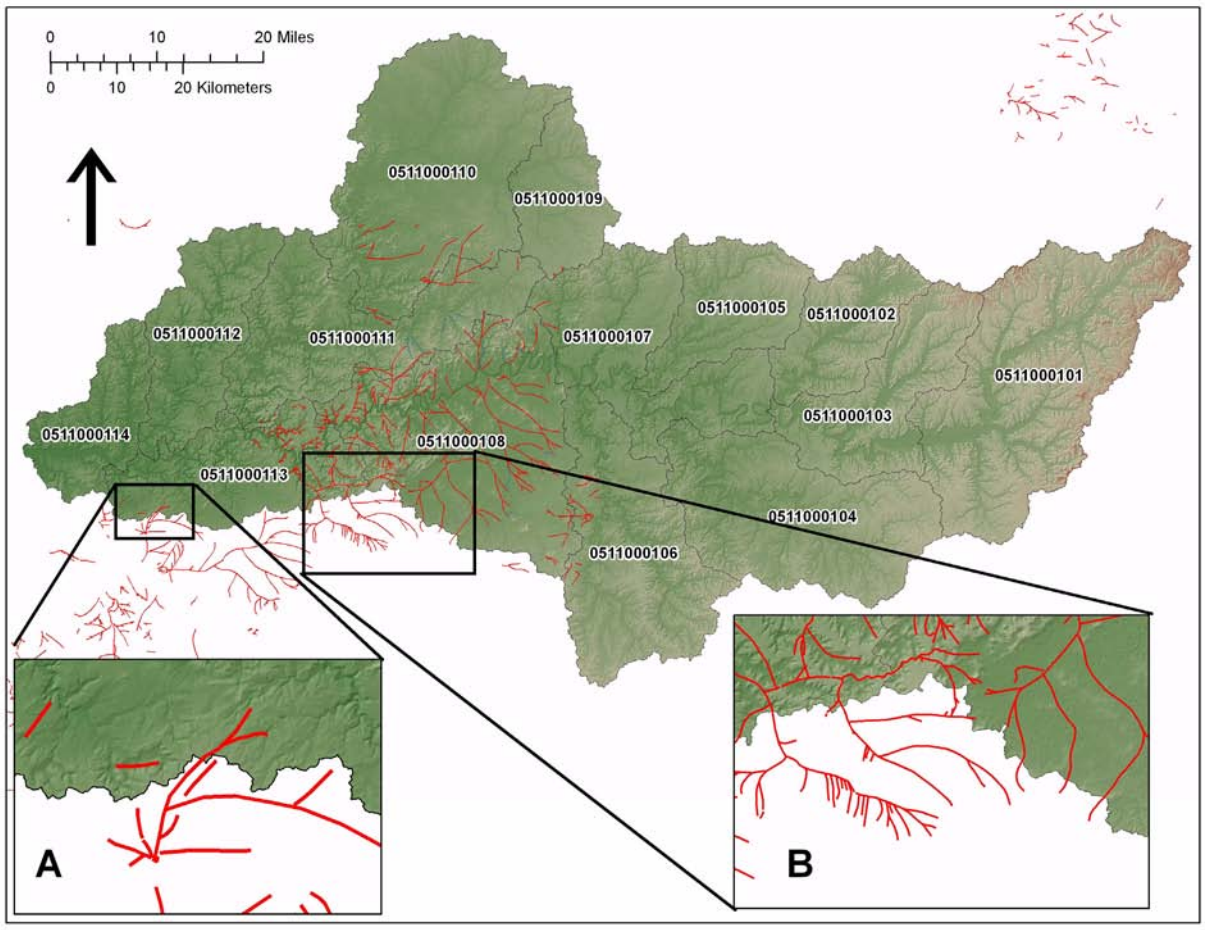

Figure 3. Processed DEM of the Upper Green River watershed (8-digit HUC 05110001), Kentucky, showing 10-digit HUs (sub-watersheds) and overlaid dye-tracer flow paths. Dye-tracer flow paths in (A) identify sinkhole drainage areas in a 10-digit HU (0511000113) mapped within the boundaries of the Upper Green River watershed that actually contribute to an adjacent 10-digit HU (not shown) located outside of the Upper Green River watershed. In contrast, dye-tracer flow paths in (B) identify a large area (approximately 85 square miles.) of sinkhole drainage mapped outside the boundaries of the Upper Green River watershed that, in fact, contribute to the watershed.

DEM PROCESSING TO MAP SINKHOLE CATCHMENTS

Sinkhole location maps have been, or are being, prepared by various State agencies in the regional study area; however, different sinkhole identification and mapping criteria are being used and the catchment areas of the sinkholes are usually not delineated. In karst terranes, delineation of sinkhole catchment areas is equally if not more important to hydrologic or water-quality studies and assessments as delineation of surface-stream watersheds. For this regional study, individual sinkhole catchment areas define useful "subbasins" within the 10-digit HUs. Therefore, a method of GIS processing of DEM data sets was developed to standardize and partly automate the mapping of sinkhole catchment areas. Topographic depressions in the DEMs are identified and artificially filled using GIS-processing tools, and a grid of the difference between the filled and unfilled depressions is developed. "Throats," or locations within the depressions that are internally drained, are identified using a GIS "SINK" tool. Grid cells associated with these throats are grouped together by assigning them unique numeric values that lump throats together into clusters and tie the clusters to an associated topographic depression. Grouped topographic depressions and throats are then used as input data to define sinkhole catchment areas using a GIS "WATERSHED" delineation tool (fig. 4A). The grouping process helps eliminate over-tessellation (subdivision) of catchment areas for depressions identified in the raster grid (fig. 4B) and helps to produce more physically realistic delineations of sinkhole catchments, complex sinkholes, and the watersheds of sinking streams that terminate in a sinkhole depression. Additional processing techniques, such as setting filters on depression size (area) and buffers near surface streams and performing cross-checks with sinkholes identified on available State maps, are needed to eliminate depressions in the raster grid that are not likely to be actual dissolution-generated sinkhole features.

RELIC STREAM VALLEYS

One unique component of the GIS processing being done for the regional study is the delineation of relic stream valleys, which are also called paleovalleys (Thrailkill, 1985). Relic stream valleys are karst geomorphic features identifiable as alignments or "trains" of sinkholes sometimes co-located within shallow topographic valleys and often appear to be the downstream extensions of sinking or losing stream reaches. Relic stream valleys represent former surface-stream channels in which flow was abandoned as a result of subsurface conduit piracy. In this study, relic stream valleys are being delineated using a GIS approach similar to that described by Glennon and Groves (2002) in which the DEMs are processed so that traces of the former surface-flow routes develop as sinkhole depressions are artificially filled to their spillover points (figs. 5A and 5B).

The identification and mapping of relic stream valleys using GIS is a potentially important outcome of this regional study because these features are often associated with the locations of major karst conduits and karst drainage basins (Thrailkill, 1985). The trends and geomorphic characteristics of the relic stream valleys also provide clues that are helpful in conceptualizing the pre-karst drainage history and in understanding the development of conduit networks and the directions of subsurface flow revealed by dye-tracer tests (fig. 6). In addition, identification and mapping of relic stream valleys may help to identify potential flood hazard areas in the region's karst terranes. Flooding of relic stream valleys—as with sinking or losing streams—occurs when the drainage capacity of sinkholes, swallets, or karst conduits cannot accommodate the volume of stormwater runoff generated within the surface catchment area (Ray, 2001). This mechanism has been identified in at least one location in the regional study area where flooding of a relic stream valley has resulted in substantial property damage (Bayless and others, 1994), and it may be an important, but poorly recognized, potential karst hazard elsewhere.

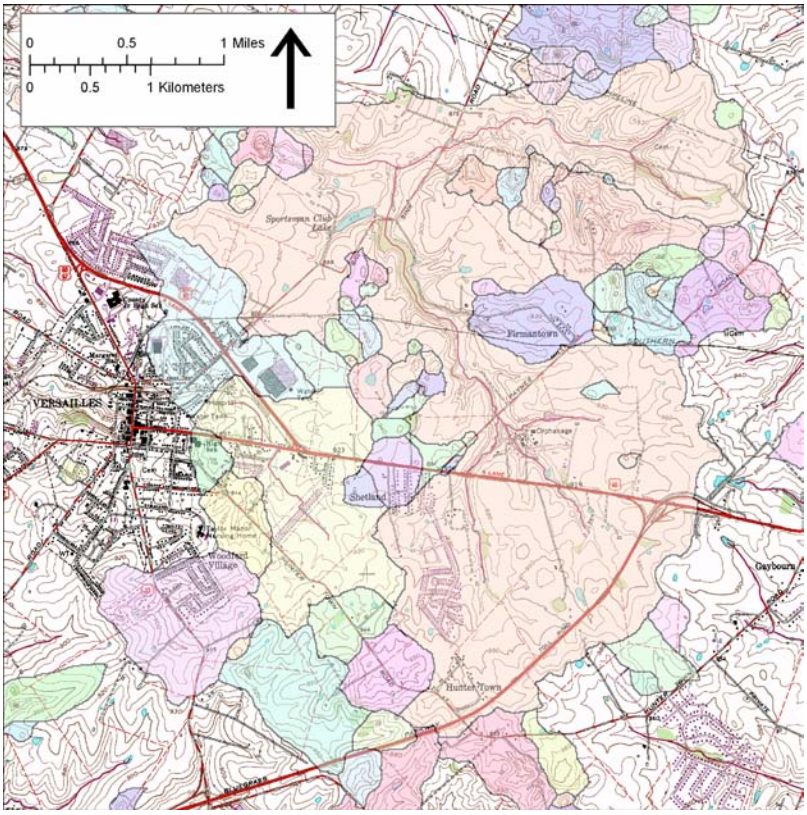

Figure 4A. Delineation of sinkhole catchments (shaded or colored polygons) near Versailles, Kentucky, (Inner Bluegrass karst terrane) using GIS-processed DEM data. The image shows the more realistic delineation of sinkhole catchments achieved by grouping "throats" (grid cells with internal drainage) within topographic depressions prior to applying the "WATERSHED" delineation tool.

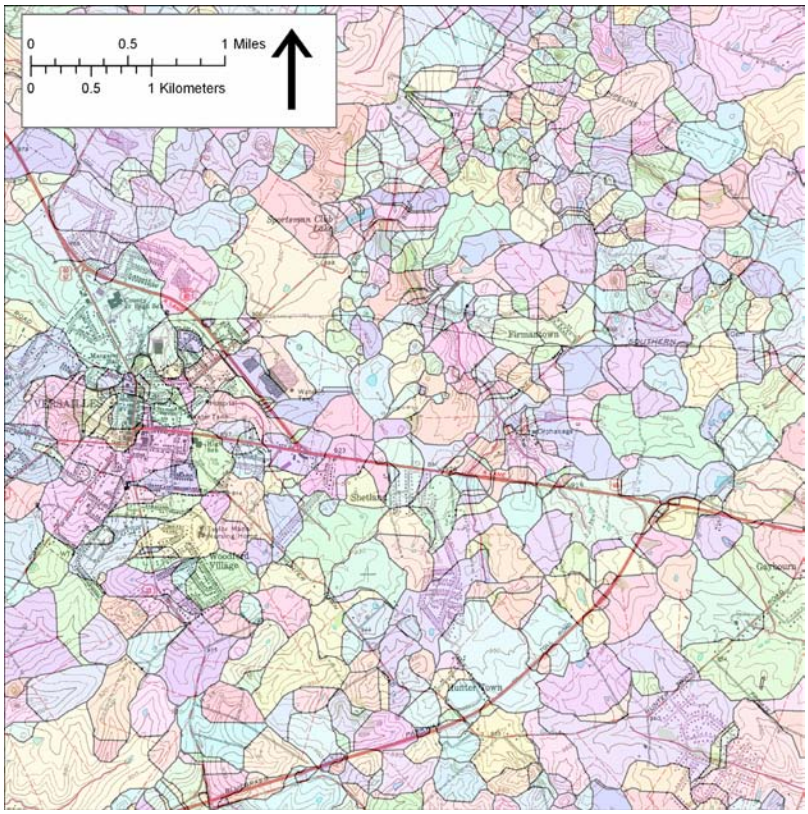

Figure 4B. Delineation of sinkhole catchments in the same area as that shown in figure 4A, illustrating the over-tessellation obtained by applying the "WATERSHED" delineation tool without grouping "throats."

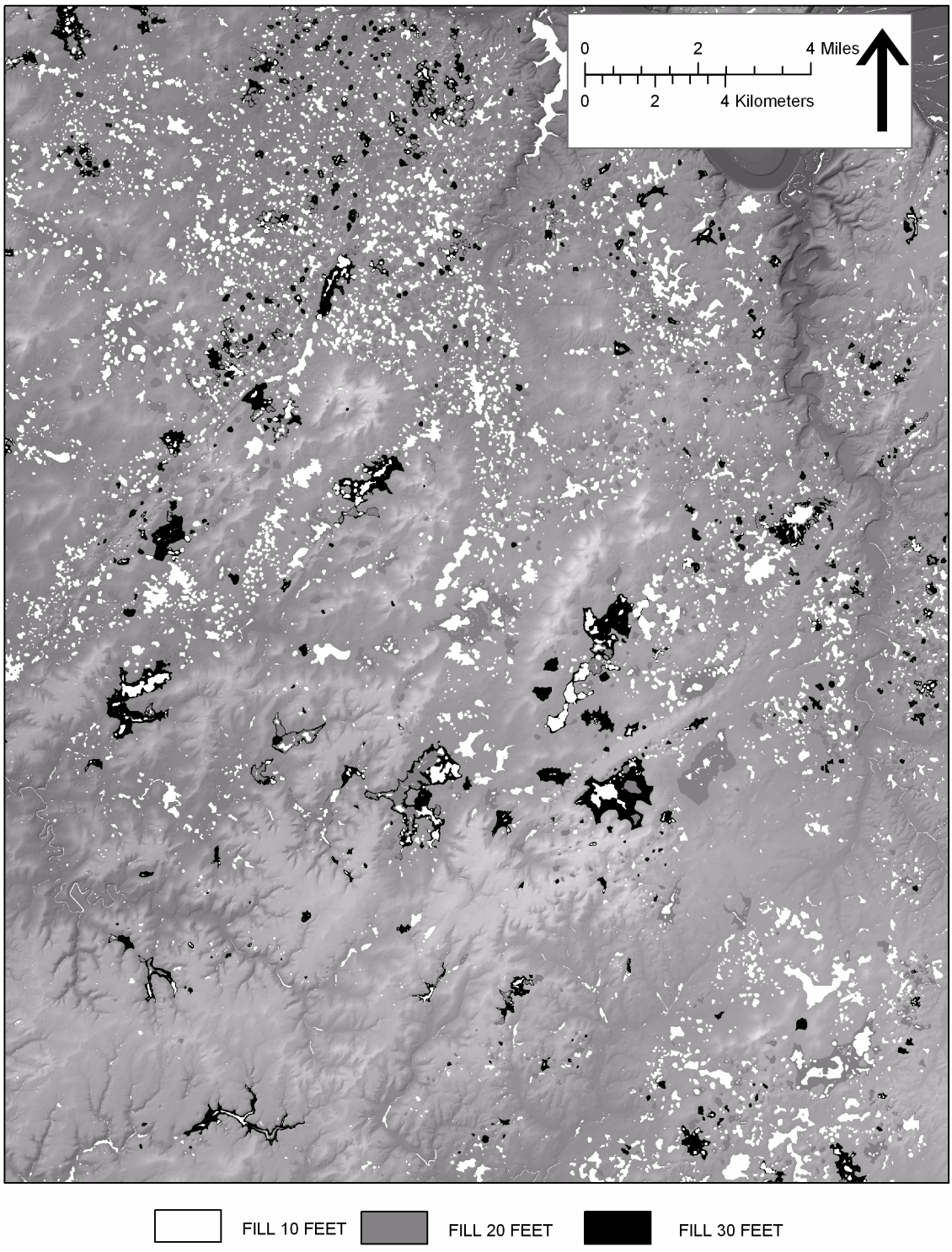

Figure 5A. Example of DEM processing used to delineate relic stream valleys in part of the Central Kentucky karst terrane. The image shows the geomorphologic patterns obtained by artificially filling identified sinkhole depressions to three different depths (indicated by shading).

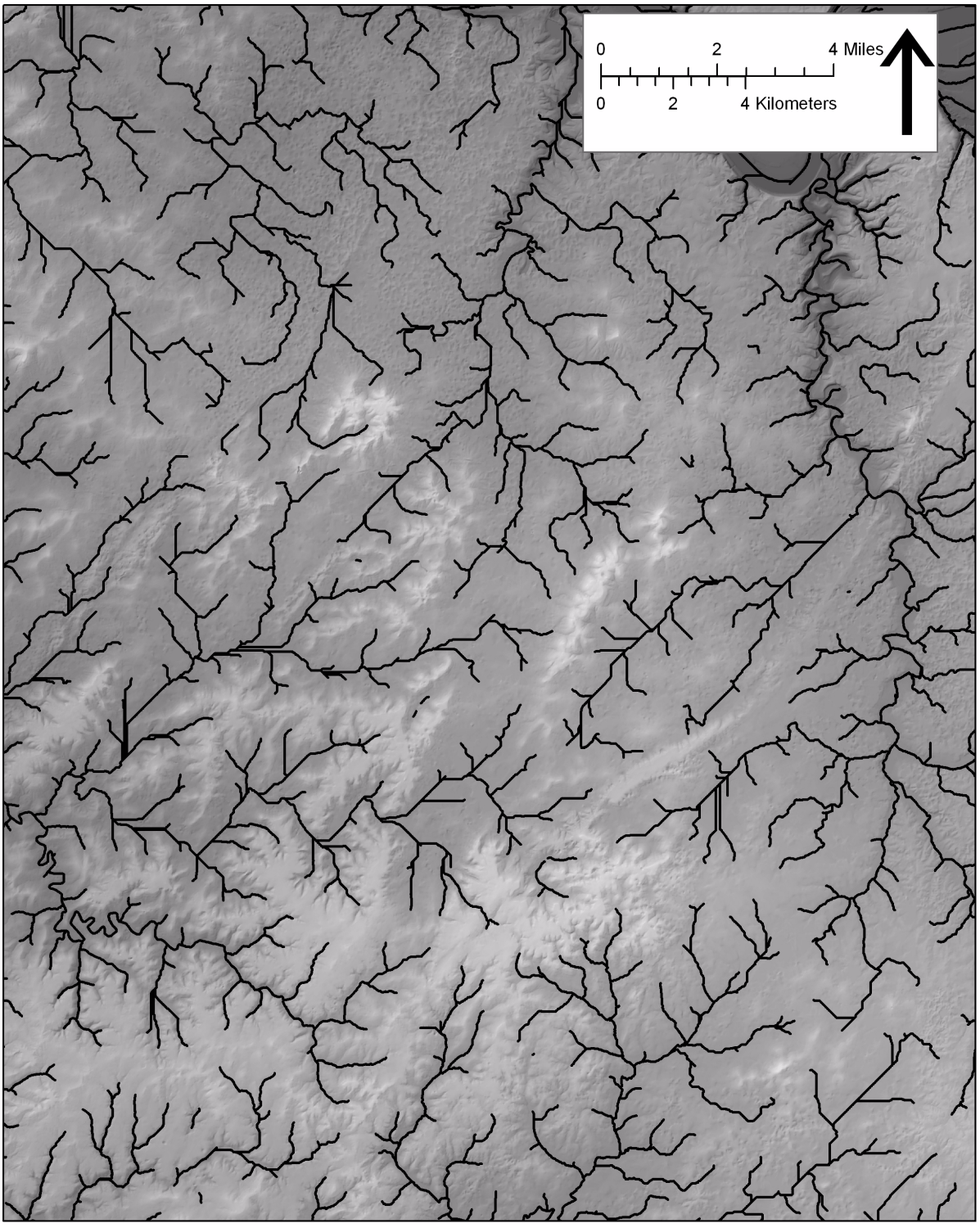

Figure 5B. Example of DEM processing used to delineate relic stream valleys in part of the Central Kentucky karst terrane. The image shows the surface-flow routes generated by artificially filling all sinkhole depressions depicted in figure 5A to their spillover points. In GIS, these flow routes—which delineate potential relic stream valleys—are overlaid and compared with the "blue-line" streams data coverage to discriminate them from present-day valleys having actively flowing surface streams.

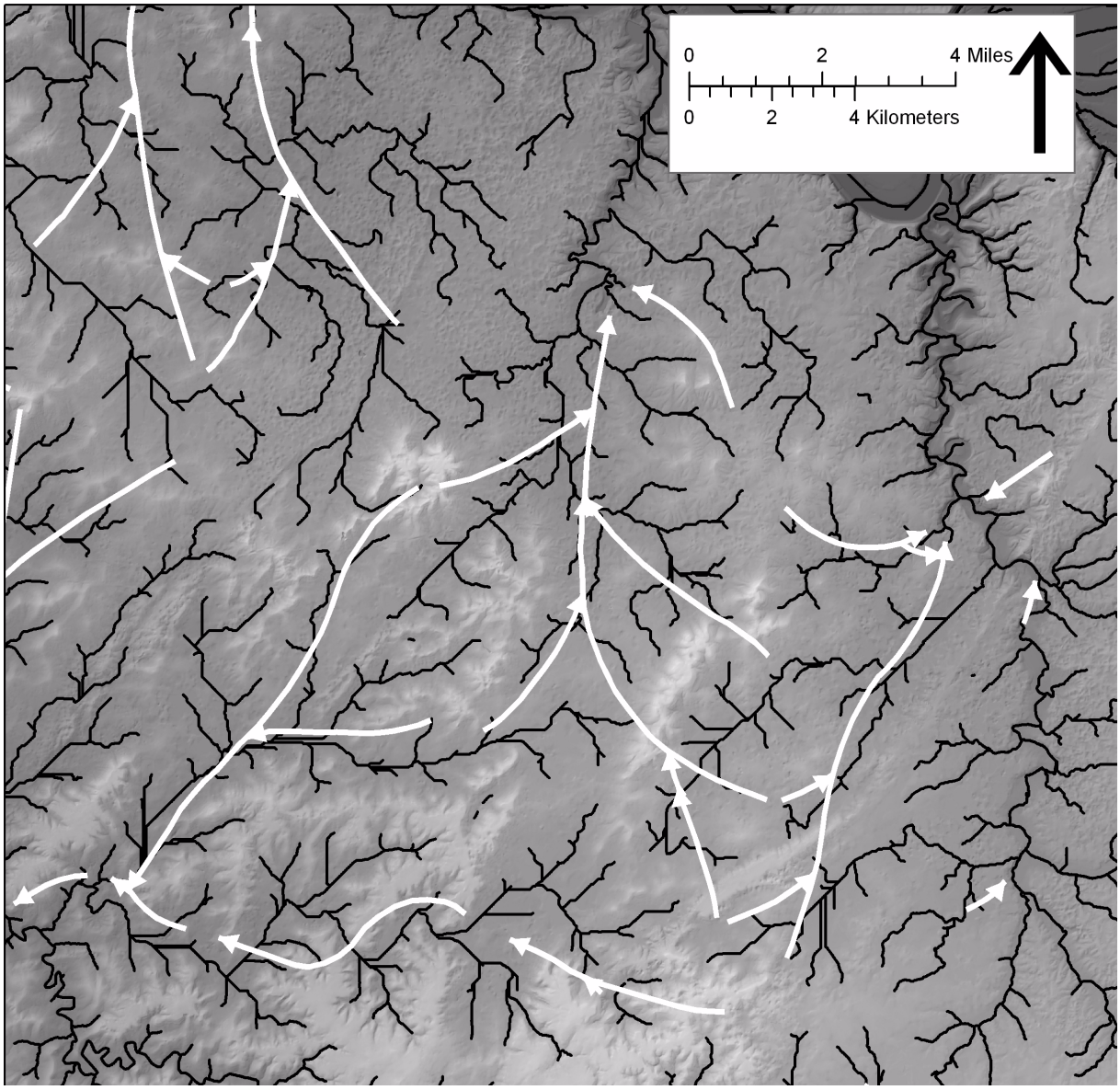

Figure 6. GIS-processed image showing the apparent relation between relic stream valleys shown in figure 5B and subsurface-flow routes inferred from results of previously published dye-tracer tests (Taylor and McCombs, 1998). The curvilinear arrows that represent the dye-tracer flow paths were drawn to follow the configuration of the potentiometric surface mapped in 1997-98 and were not altered to follow the GIS-generated trends for the relic stream valleys.

REFERENCES

Bayless, E.R., Taylor, C.J., and Hopkins, M.S., 1994, Directions of ground-water flow and locations of ground-water divides in the Lost River watershed near Orleans, Indiana: U.S. Geological Survey Water-Resources Investigations Report 94-4195, 25 p., 2 pls.

Currens, J.C., and Ray, J.A., 1999, Karst atlas for Kentucky, *in* Beck, B.F., Pettit, A.J., and Herring, J.G., eds., Hydrogeology and engineering geology of sinkholes and karst—Proceedings of the Seventh Multidisciplinary Conference on Sinkholes and the Engineering and Environmental Impacts of Karst, April 10-14, 1999: Harrisburg-Hershey, Penn., A.A. Balkema, Rotterdam, Holland the Netherlands, p. 85-90.

Florea, L.J., Paylor, R.L., Simpson, L., and Gulley, J., 2002, Karst GIS advances in Kentucky: Journal of Cave and Karst Studies, v. 64, no. 1, p. 58-62.

Gao, Y., 2002, Karst feature distribution in southeastern Minnesota—Extending GIS-based database for spatial analysis and resource management: Minneapolis, University of Minnesota, Ph.D. dissertation, 210 p.

Glennon, A., and Groves, C., 2002, An examination of perennial stream drainage patterns within the Mammoth Cave watershed, Kentucky: Journal of Cave and Karst Studies, v. 64, no. 1, p. 82-91.

Quinlan, J.F., and Ewers, R.O., 1989, Subsurface drainage in the Mammoth Cave area, *in* White, W.B., and White, E.L., eds., Karst hydrology concepts from the Mammoth Cave area: Van Nostrand Reinhold, New York, p. 65-104.

Ray, J.A., 2001, Spatial interpretation of karst drainage basins, *in* Beck, B.F., ed., Geotechnical and environmental applications of karst geology and hydrology—Proceedings of the Eighth Multidisciplinary Conference on Sinkholes and the Environmental and Engineering Impacts of Karst, April 1-4, 2001: Louisville, Ky., Swets & Seitlinger, Lisse, Holland the Netherlands, p. 235-244.

Ray, J.A., Goodmann, P.T., and Meiman, J., 2000, Hydrologically valid delineation of watershed boundaries in Kentucky's karst terrane, *in* Proceedings of the Eighth Mammoth Cave Science Conference: Mammoth Cave National Park, p. 75-76.

Taylor, C.J., and McCombs, G.K., 1998, Recharge-area delineation and hydrology, McCraken Springs, Fort Knox Military Reservation, Meade County, Kentucky: U.S. Geological Survey Water-Resources Investigations Report 98-4196, 12 p., 1 pl.

Thrailkill, J., 1985, The Inner Bluegrass karst region, *in* Dougherty, P.H., ed., Caves and Karst of Kentucky: Kentucky Geological Survey Special Publication 12, Series IX, p. 28-62.

Veni, G., 1999, A geomorphological strategy for conducting environmental impact assessments in karst areas: Geomorphology, v. 31, p. 151-180.

Veni, G., 2003, GIS applications in managing karst groundwater and biological resources, *in* Beck, B.F., ed., Sinkholes and the engineering and environmental impacts of karst—Proceedings of the Ninth Multidisciplinary Conference, September 6-10, 2003: Huntsville, Ala., American Society of Civil Engineers Geotechnical Special Publication No. 122, p. 466-474.

Application of Multiple Tracers to Characterize Complex Sediment and Pathogen Transport in Karst

Tiong Ee Ting[1], Ralph K. Davis[2], J. V. Brahana[2], P.D. Hays[2,3], and Greg Thoma[1]
[1]Department of Chemical Engineering, 3202 Bell, University of Arkansas, Fayetteville, AR 72701
[2]Department of Geosciences, 113 Ozark, University of Arkansas, Fayetteville, AR 72701
[3]US Department of Agriculture, National Water Management Center, 44 Ozark, Fayetteville, AR 72701

ABSTRACT

Injections of multiple tracers were conduced to characterize ground-water flow, sediment transport, and *E. coli* transport in a mantled-karst aquifer under variable flow conditions at the Savoy Experimental Watershed. Rhodamine WT and fluorescein, used as conservative tracers in this study, were injected two hours after the injection of lanthanum-labeled clay and europium-labeled *E.coli* into a losing-stream reach under a natural hydraulic gradient. The injection occurred on the recessional limb of a major storm pulse, and fate and transport of the tracers were observed for multiple tests under varying hydrologic conditions using multiple tracers for two springs of an underflow/overflow spring complex. The underflow spring, Langle, is located approximately 490 meters in a straight-line direction from the injection point, in a different surface-water catchment than the losing stream. The major overflow spring, Copperhead, is 453 meters in a straight-line from the injection point, and it lies in the same surface-water catchment as the losing stream. The altitude of the resurgence of Langle Spring is about 3 centimeters less than the resurgence of Copperhead Spring, based on multiple surveys using a total station.

Results from the tracer breakthrough for near steady-state conditions showed the arrival of suspended sediment and *E. coli* at 10.7- and 5.9 hours respectively before the conservative dye tracers at Langle Spring. The early arrival of sediment and *E. coli* is hypothesized to result from gravitational settling velocity coupled with the effect of pore-size exclusion. The conservative dye tracers arrived first at Copperhead Spring, followed by *E. coli* and sediment, essentially a reversal of the sequence at Langle Spring. During later storm-induced tracer tests, all tracers were observed to arrive simultaneously at each spring, with Copperhead Spring, along the shorter flow path, receiving the tracer pulses about an hour before Langle Spring. This and other tracer tests in this overflow/underflow system suggest that sediment and *E. coli* are stored in pools in the subsurface. These pools provide continuous full-conduit flow to Langle, the underflow spring, and only partially-full conduit flow to Copperhead, the overflow spring. However, during high flows associated with transient storm events, the tracers are flushed from ephemeral storage in the pools and move as a pulse associated with the rising limb of the hydrograph. The application of multiple tracers proved to be an invaluable tool in providing mechanisms to fully characterize the subsurface flow.

Estimating Ground-Water Age Distribution from CFC and Tritium Data in the Madison Aquifer, Black Hills, South Dakota

By Andrew J. Long and Larry D. Putnam
U.S. Geological Survey, 1608 Mountain View Rd, Rapid City, South Dakota 57702

Abstract

Ground-water age distribution was estimated for water collected from a well in the karstic Madison aquifer in the Black Hills of South Dakota using a ground-water mixing model for chlorofluorocarbon (CFC) and tritium data. Input functions for the model included precipitation concentrations for four tracers—CFC12, CFC11, CFC113 (6-month data), and tritium (yearly data). Madison aquifer water often is a complex mixture of waters of various ages; however, existing ground-water age-dating methods generally are not well suited for estimating the unique age distributions of ground water that can occur in karst aquifers. CFC data alone often can provide estimates of piston-flow ages or binary mixtures of young and old water, but generally are inadequate for estimating age distributions at a finer time discretization. However, if a time series of tritium data is incorporated into an age-dating model along with CFC data, an age distribution discretized to a 6-month time step can be estimated with statistical significance by assuming that ground-water age fits a probability density function (PDF). This method estimates one age distribution that satisfies all of the combined tracer data and thus has two advantages. The first of which is that the number of measured values applied to a single problem is maximized, which helps to constrain the solution, and second is that confidence in the solution is increased if a single solution satisfies more than one type of data. The PDF indicates the estimated fraction of water at a site for each 6-month age category. Because results from multiple age-dating tracers should agree, and because together they may provide complimentary information, combining all of the data into one model can be a powerful method for describing the history of recharge to a well or spring.

The best fit of CFC and tritium data for samples from a municipal water supply well open to the Madison aquifer was a bimodal age distribution, which was a composite of a uniform and a lognormal PDF. Data used in the model included the concentrations for each of the 3 CFCs (1 sample) and a time series of tritium concentrations (4 samples over 10 years). These samples provided a total of 7 tracer concentrations, which were compared to the corresponding modeled values. Parameter optimization methods, which minimize the residuals of measured and modeled values, were used to estimate the 4 parameters that describe the bimodal age distribution. Because there were 7 measured tracer concentrations and only 4 parameters to be estimated, the solution was adequately constrained, and the parameters could be estimated with reasonable confidence. Results indicated that about 33 percent of the mixture was less than 2 years old (uniform PDF component), 5 percent was 10 to 30 years old (lognormal PDF component), and the remaining 62 percent was more than 50 years old. Because CFC and tritium concentrations in precipitation were very low before 1950, the age distribution of water more than about 50 years old could not be estimated. The bimodal age distribution was the only distribution tested that could explain the combined CFC and the tritium data with acceptable 95-percent confidence limits on the estimated parameter values.

A Multi-Tracer Approach for Evaluating the Transport of Whirling Disease to Mammoth Creek Fish Hatchery Springs, Southwestern Utah

By Lawrence E. Spangler[1], Meiping Tong[2], and William Johnson[2]
[1]U.S. Geological Survey, 2329 Orton Circle, Salt Lake City, Utah 84119
[2]Department of Geology and Geophysics, University of Utah, Salt Lake City, Utah 84112

ABSTRACT

The Utah Division of Wildlife Resources has been concerned about the vulnerability of selected spring-fed fish hatcheries to whirling disease caused by the microscopic parasite *Myxobolus cerebralis*. Whirling disease is typically transmitted from one water body to another by birds or fishermen but can potentially migrate along underground flow paths in areas where aquifer permeability is high and ground-water movement is rapid enough to allow passage and survival of the parasite. Mammoth Creek Fish Hatchery in southwestern Utah tested positive for whirling disease in 2002. Because adjacent Mammoth Creek also tested positive, a study was begun to evaluate potential hydrologic connections between the creek, an irrigation canal off the creek, and the hatchery springs.

Dye-tracer studies indicate that water lost through the channel of Mammoth Creek discharges from the west and east hatchery springs. Ground-water time of travel to the springs was about 7.5 hours, well within the 2-week timeframe of viability of the parasite. Results of studies using soil bacteria and club moss spores as surrogate particle tracers indicate that the potential for transport of the parasite through the fractured basalt may be low. Bacteria concentrations in spring water generally were below reporting limits, and club moss spores were recovered from only a few samples. However, peak concentrations for the bacteria and club moss spores in water from the east hatchery spring coincided with peak dye recovery. No particle tracers were recovered from the west hatchery spring.

INTRODUCTION

The Utah Division of Wildlife Resources operates 10 fish hatcheries in Utah that use water from large springs and has been concerned about the vulnerability of these hatcheries to whirling disease caused by the microscopic parasite *Myxobolus cerebralis.* Whirling disease is typically transmitted from one water body to another by birds or fishermen. However, the triactinomyxon spores (TAMs) produced by the parasite can potentially migrate along underground flow paths in areas where aquifer permeability is high, such as in karst and volcanic terrains, and the movement of ground water is sufficiently rapid to allow viable passage of the spores.

In 2000, whirling disease was detected in the Midway Fish Hatchery, about 30 miles (mi) southeast of Salt Lake City. Results of investigations by Carreon-Diazconti and others (2003) showed that the likely source of the parasite in the spring water supplying the hatchery was the Provo River. Water diverted from the river, which also tested positive for the disease, was used to irrigate farmland upgradient from the hatchery and subsequently moved downward into the karst (travertine) aquifer supplying the springs. Use of cultured soil bacteria as a surrogate tracer for the parasite showed that transport of the spore to the springs through open conduits and fractures in the limestone was possible (Stephen Nelson and Alan Mayo, Brigham Young University, written commun., 2000).

In 2002, Mammoth Creek Fish Hatchery in southwestern Utah became the second State- operated facility to become infected by whirling disease. Because adjacent Mammoth Creek also tested positive, the U.S. Geological Survey, in cooperation with the Utah Division of Wildlife Resources, began a study to evaluate potential hydrologic connections and determine ground-water travel times between the creek, an irrigation canal off the creek, and the

hatchery springs, and to assess the potential for transport of the parasite along underground flow paths to the springs. This paper summarizes the results of tracer studies.

DESCRIPTION OF STUDY AREA

Mammoth Creek State Fish Hatchery is located about 2 mi southwest of Hatch, Utah, at the mouth of Mammoth Creek Valley, at an altitude of 7,000 feet (ft) (fig. 1). The hatchery is situated at the base of a 40-ft-high basalt cliff, from which two major (west and east) springs discharge. Total discharge of the springs averages about 3 cubic feet per second (ft^3/sec), with a variability of less than 1 ft^3/sec. Flow from the springs is diverted through the hatchery for fish-rearing operations and is then discharged into Mammoth Creek, which flows past the hatchery. McCormick spring also discharges from near the base of the basalt cliff about 750 ft northeast of the hatchery springs, on private land (fig. 1). Discharge of this spring was about 50 gallons per minute (gpm) during the study and appeared to be fairly constant. Bonanza spring emerges from talus alongside the channel of Mammoth Creek about 1,200 ft upstream from the hatchery (fig. 1) and discharged about 40 gpm. Discharge of this spring was observed to vary with changes in streamflow in Mammoth Creek.

During the summer, water is diverted from Mammoth Creek into a canal about 2 mi west of the hatchery (fig. 1) for irrigation in the lower part of the valley. During the study, all water from the creek was diverted into the canal and only a small amount of inflow from springs was observed downstream in the channel, which subsequently was lost through the streambed (fig. 2).

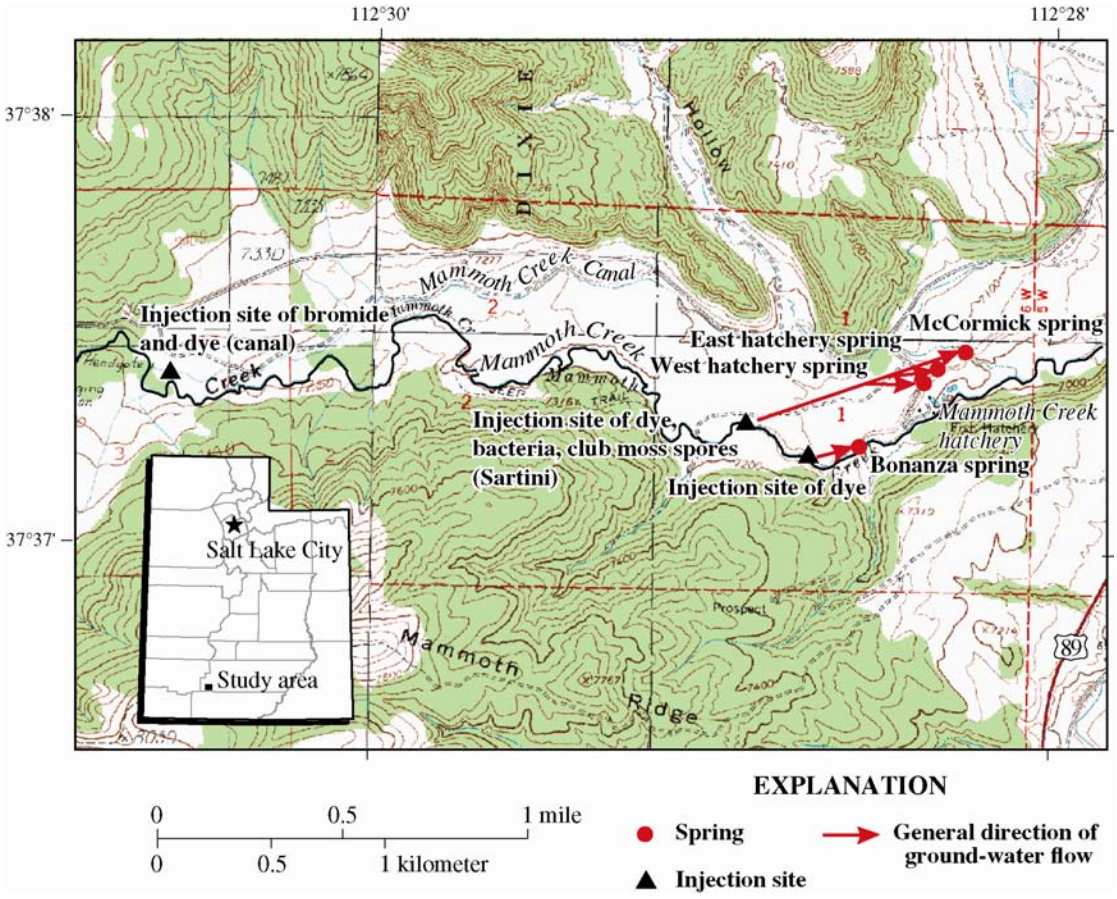

Figure 1. Location of injection sites and springs and general directions of ground-water movement in the Mammoth Creek study area, southwestern Utah.

Quaternary-age basaltic lava partly fills Mammoth Creek Valley and caps adjacent ridges. In the vicinity of the hatchery, the basalt has been entrenched by Mammoth Creek to a depth of as much as 40 ft (fig. 2). Vertical and horizontal fracturing is pervasive throughout the basalt. Limestones, marls, and calcareous shales of the Tertiary-age Claron Formation underlie the basalt and adjacent hillsides and are locally cavernous.

METHODOLOGY

Major-ion chemistry, tritium age-dating, streamflow measurements, spring discharge variability, and tracer studies were used to determine hydrologic relations in the Mammoth Creek hatchery area. Fluorescent dyes (sodium fluorescein and rhodamine WT) and sodium bromide were used to establish ground-water connections between Mammoth Creek, an irrigation canal off the creek, and the springs at, and in the vicinity of, the fish hatchery. Automatic samplers collected water directly from the springs for analysis. Dye samples were analyzed by filter fluorometry (Wilson and others, 1986). Sodium bromide samples were analyzed by ion chromatography (Fishman and Friedman, 1989). Non-pathogenic cultured soil bacteria *(Acidovorax)* and club moss *(Lycopodium)* spores were used as surrogate particle tracers to simulate the size (10 to 100 microns) and transport characteristics of the whirling disease parasite through the fractured basalt aquifer. Bacteria samples were collected manually in centrifuge vials, magnetically tagged, and analyzed by ferrographic techniques (Johnson and McIntosh, 2003). Club moss spores were collected in plankton nets (fig. 3), isolated by filtration, and analyzed by standard microscopic techniques (Gardner and Gray, 1976).

RESULTS AND DISCUSSION

On the basis of dye-tracer tests completed in October 2002 and October 2003 (table 1), water lost through the channel of Mammoth Creek about 3,000 ft southwest of the hatchery (at Sartini) discharges from the west and east hatchery springs and from McCormick spring (fig. 1). However, water lost through the channel farther downstream appears

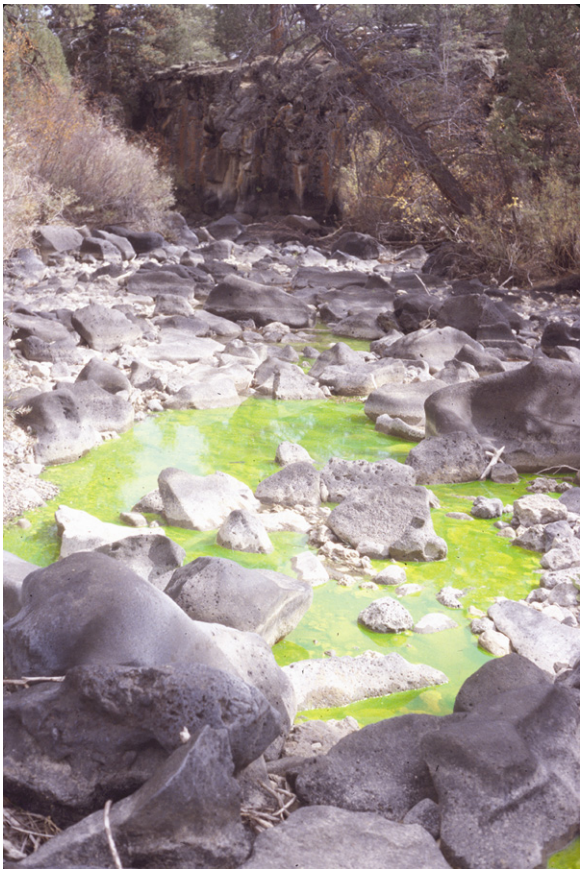

Figure 2. Mammoth Creek channel at the Sartini tracer-injection site, looking downstream. Surface water seeps into the streambed and appears to move along fractures within the basalt to the springs.

Figure 3. Plankton nets were used to collect club moss spores from the west and east hatchery springs. Spores were used as surrogate tracers (33 microns) for the whirling disease parasite.

Table 1. Summary of tracer injections in the Mammoth Creek study area, southwestern Utah.

[g, grams; kg, kilograms; —, no data]

Tracer-injection site	Date-time of tracer injection		Type of tracer	Amount of tracer	Tracer-recovery site	Date-time of tracer recovery (first arrival)		Travel time to first arrival (hours)	Linear distance (feet)
Mammoth Creek	10/02/02	1300	Rhodamine WT dye	1 liter	Bonanza spring	10/02/02	2015	[1]7.25	750
Mammoth Creek at Sartini	10/12/02	1300	Fluorescein dye	454 g	Hatchery springs (combined)	10/12/02	2300	10	2,800
					McCormick spring	10/13/02	1100	[2]22	3,300
Mammoth Creek at Sartini	10/09/03	1630	Rhodamine WT dye	1 liter	West hatchery spring	10/10/03	0000	7.5	2,800
					East hatchery spring	10/10/03	0100	8.5	3,000
					McCormick spring	10/10/03	1045	[3]18.25	3,300
	10/09/03	1615	Bacteria (OY-107 strain)	10^{14} cells	East hatchery spring	10/10/03	0700	[4]14.75	3,000
	10/09/03	1645	Club moss spores	1 kg	East hatchery spring	10/10/03	1205	[5]19.25	3,000
Mammoth Creek canal	10/10/02	1340	Sodium bromide	25 kg	No recovery	—	—	—	—
	10/11/02	1720	Sodium bromide	25 kg	No recovery	—	—	—	—
Mammoth Creek canal	07/31/03	2200	Fluorescein dye	1.36 kg	McCormick spring	08/19/03	1700	[6]451	[7]—

[1]Samples collected downstream of spring; maximum travel time.
[2]Samples collected daily; maximum travel time.
[3]Samples collected twice daily; maximum travel time.
[4]Recovered near peak dye concentration; maximum travel time.
[5]Represents composite sample over previous 13.5 hours.
[6]Dye recovered on activated charcoal; maximum travel time.
[7]Exact location of loss zone along canal unknown.

to discharge only from Bonanza spring. Ground-water travel time (first arrival) from Mammoth Creek (at Sartini) to the west hatchery spring was about 7.5 hours with a lag of about 1 hour between the west and east springs (fig. 4). Time to peak dye concentration (about 7 parts per billion) occurred about 8 hours after first arrival. Total dye-mass recovery for both springs was about 22 percent of that injected.

Ground-water movement from Mammoth Creek to the hatchery springs appears to be along flow path(s) that are separate from those to Bonanza spring and are probably related to fracturing within the basalt. However, because water from the hatchery springs and McCormick spring discharges from multiple outlets along the same horizon, flow appears to be, at least in part, along lateral zones of high permeability within the basalt. These zones could include horizontal fractures, interflow horizons between successive lava flows, or possibly the contact between the base of the basalt and the original valley floor.

Although pathways of rapid ground-water flow exist between the losing reach along Mammoth Creek and the hatchery springs, low variability in spring flow indicates that this is probably a small component of total discharge and that average ground-water travel time within the aquifer is likely to be considerably longer. The concentration of tritium (15.4 picocuries per liter) in water from the west hatchery spring indicates, however, a substantial component of modern (post-1960s) water.

Results of dye-tracer studies indicate that ground-water time of travel between Mammoth Creek and the west and east hatchery springs is well within the 2-week timeframe of viability of the whirling disease parasite. However, results of studies using bacteria and club moss spores as surrogate tracers to simulate the size and movement of the parasite underground indicate that the potential for transport of the parasite through the fractured basalt aquifer from the creek may be low. Bacteria concentrations in water samples from the springs generally were below reporting limits (less than 10 cells per milliliter), and club moss spores were recovered from only a few samples. Substantial losses of the particle tracers probably occurred during infiltration through the streambed sediments and during transport within the aquifer.

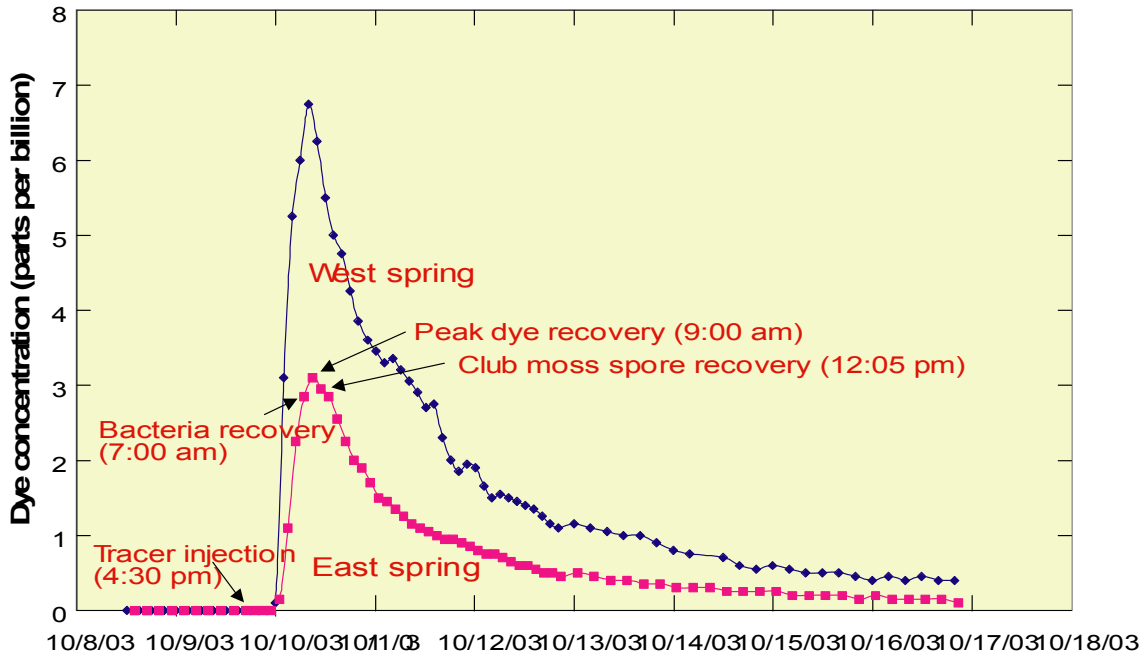

Figure 4. Rhodamine WT dye-recovery curves, and bacteria and club moss spore peak recoveries for the east hatchery spring. No particle tracers were recovered from the west hatchery spring.

Although the vast majority of particle tracers were not recovered, peak concentrations for the bacteria (about 10 cells per milliliter) and club moss spores (about 60 spores per milliliter) in water from the east hatchery spring coincided with peak dye recovery (fig. 4). No particle tracers were recovered from the west hatchery spring.

Streamflow measurements along the irrigation canal off Mammoth Creek showed substantial losses along selected reaches, particularly in the upper part of the canal (fig. 1). Measured streamflow losses along a 2-mi reach below the diversion were as much as 2 ft^3/sec, or about 22 percent of the flow. Bromide and dye tracers injected in the canal just below the diversion in October 2002 and July 2003, respectively, were not detected at the hatchery springs, but dye was detected at McCormick spring (table 1). Non-detection of the tracers at the hatchery springs probably resulted from dispersion and dilution within the matrix of the basalt aquifer, resulting in ground-water travel times greater than the 6-week monitoring period and (or) tracer concentrations below the detection limits. Although water lost along the upper reaches of the canal probably discharges at the hatchery springs, ground-water travel times likely exceed the timeframe of viability for transport of the parasite through the basalt.

SUMMARY

Dye-tracer studies at the Mammoth Creek Fish Hatchery indicate that water lost through the channel of Mammoth Creek discharges from the west and east hatchery springs. Ground-water time of travel to the springs was about 7.5 hours, well within the 2-week timeframe of viability of the whirling disease parasite. However, results of studies using soil bacteria (*Acidovorax*) and club moss (*Lycopodium*) spores as surrogate particle tracers for the parasite indicate that the potential for transport through the fractured basalt from the creek may be low. Substantial losses of the particle tracers occurred during streambed infiltration and aquifer transport. Bacteria concentrations generally were below reporting limits and club moss spores were recovered from only a few samples. However, peak concentrations for the bacteria and club moss spores in water from the east hatchery spring coincided with peak dye recovery. No particle tracers were recovered from the west hatchery spring. In addition, bromide and dye tracers injected in an irrigation canal were not detected at the hatchery springs.

REFERENCES

Carreon-Diazconti, C., Nelson, S.T., Mayo, A.L., Tingey, D.G., and Smith, M., 2003, A mixed groundwater system at Midway, Utah: Discriminating superimposed local and regional discharge: Journal of Hydrology, v. 273, p. 119-138.

Fishman, M.J., and Friedman, L.C., 1989, Methods for determination of inorganic substances in water and fluvial sediments: U.S. Geological Survey Techniques of Water-Resources Investigations, Book 5, Chap. A1, 545 p.

Gardner, G.D., and Gray, R.E., 1976, Tracing subsurface flow in karst regions using artificially colored spores: Bulletin of the Association of Engineering Geologists, v. 13, no. 3, p. 177-197.

Johnson, W.P., and McIntosh, W.O., 2003, Tracking of injected and resident (previously injected) bacterial cells in groundwater using ferrographic capture: Journal of Microbiological Methods, v. 54, p. 153-164.

Wilson, J.F., Jr., Cobb, E.D., and Kilpatrick, F.A., 1986, Fluorometric procedures for dye tracing: U.S. Geological Survey Techniques of Water-Resources Investigations, Book 3, Chap. A12, 34 p.

National Evaporite Karst--Some Western Examples

By Jack B. Epstein
U.S. Geological Survey, National Center, MS 926A, Reston, VA 20192

ABSTRACT

Evaporite deposits, such as gypsum, anhydrite, and rock salt, underlie about one-third of the United States, but are not necessarily exposed at the surface. In the humid eastern United States, evaporites exposed at the surface are rapidly removed by solution. However, in the semi-arid and arid western part of the United States, karstic features, including sinkholes, springs, joint enlargement, intrastratal collapse breccia, breccia pipes, and caves, locally are abundant in evaporites. Gypsum and anhydrite are much more soluble than carbonate rocks, especially where they are associated with dolomite undergoing dedolomitization, a process which results in ground water that is continuously undersaturated with respect to gypsum. Dissolution of the host evaporites cause collapse in overlying non-soluble rocks, including intrastratal collapse breccia, breccia pipes, and sinkholes. The differences between karst in carbonate and evaporite rocks in the humid eastern United States and the semi-arid to arid western United States are delimited approximately by a zone of mean annual precipitation of 32 inches. Each of these two rock groups behaves differently in the humid eastern United States and the semi-arid to arid west. Low ground-water tables and decreased ground water circulation in the west retards carbonate dissolution and development of karst. In contrast, dissolution of sulphate rocks is more active under semi-arid to arid conditions. The generally thicker soils in humid climates provide the carbonic acid necessary for carbonate dissolution. Gypsum and anhydrite, in contrast, are soluble in pure water lacking organic acids. Examples of western karst include the Black Hills of South Dakota and the Holbrook Basin in Arizona. A draft national map of evaporite karst is presented here.

INTRODUCTION

The present, the map indicating engineering aspects of karst (Davies and others, 1984, scale 1:7,500,000) adequately shows the distribution of carbonate karst in the United States, but the widespread distribution of evaporite karst is inadequately portrayed. The map depicts areas of karstic rocks (limestone, dolomite, and evaporites), and pseudokarst, classified as to their engineering and geologic characteristics (size and depth of voids, depth of overburden, rock/soil interface conditions, and geologic structure).

In the eastern United States, where average annual precipitation commonly is greater than 30 inches, gypsum deposits generally are eroded or dissolved to depths of at least several meters or tens of meters below the land surface. So, although gypsum in the east may locally be karstic, the lack of exposures makes it difficult to prove this without subsurface study of the gypsum and its dissolution features. In the semi-arid western part of the United States, however, in areas where the average annual precipitation commonly is less than about 32 inches, gypsum tends to resist erosion and typically caps ridges, mesas, and buttes. In spite of its resistance to erosion in the west, gypsum commonly contains visible karst features, such as cavities, caves, and sinkholes, attesting to the importance of ground-water movement, even in low-rainfall areas. Salt karst is less common at the earth's surface than gypsum karst because it is so soluble that it survives at the surface only in very arid areas.

While the distribution of carbonate karst on the Davies' map is generally adequate, the map only depicts gypsum karst in a few areas (fig. 1). In an extensive text on the back of the map, caves and fissures in gypsum in western Oklahoma and the eastern part of the Texas Panhandle is mentioned. The

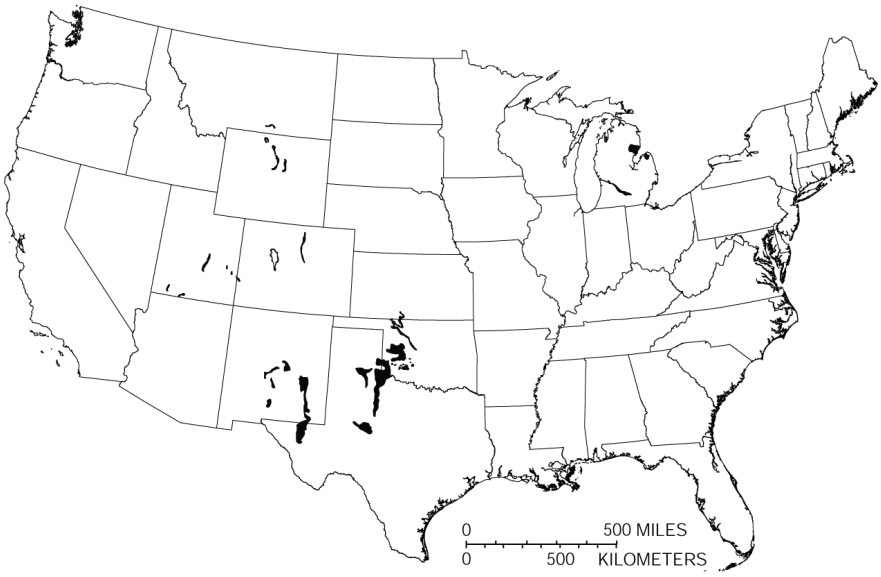

Figure 1. Map showing areas of evaporite karst in the United States, as depicted by Davies and others (1984).

map does not show the distribution of salt or salt karst even though the text mentions natural subsidence and man-induced subsidence due to solution mining in salt beds in south-central and southwestern Kansas.

Several national maps of evaporite deposits were summarized by Epstein and Johnson (2003) who prepared a map showing the present perception of evaporite distribution and evaporite karst in the United States (fig. 2). The map includes gypsum/anhydrite and halite basins, and incorporates the limited areas of evaporite karst depicted by Davies and others (1984) compared to the larger areas of the same shown by Johnson (1997). Collapse due to human activities, such as solution mining, are also shown, as well as a line of mean annual precipitation (32.5 in.) that approximates the boundary between distinctively different karst characteristics, between the humid eastern United States and the semi-arid west. Also shown are the Holbrook Basin in Arizona and the Black Hills of South Dakota and Wyoming, whose variety of surface and subsurface evaporite-karst features are described here.

HOLBROOK BASIN, ARIZONA

Many workers have reported a variety of evaporite- and carbonate-karst features in Arizona (fig. 3A) that are not found on Davies (1984) map (fig. 3B). Subsurface halite deposits were mapped by Eaton and others (1972), Johnson and Gonzales (1978), Ege (1985), and Neal and others (1998); more detailed mapping of salt deposits in the Holbrook Basin was done by Peirce and Gerrard (1966) and Rauzi (2000). An area of breccia pipes was delimited in northwest Arizona by Harris (2002); they were probably the result of collapse over carbonate rocks, but evaporite collapse could not be ruled out. Scattered gypsum and anhydrite localities were shown by Withington (1962). Comparing this composite map with the Davies map (fig. 3*B*) shows that many types of karstic features could be shown in both evaporite and carbonate rocks in Arizona.

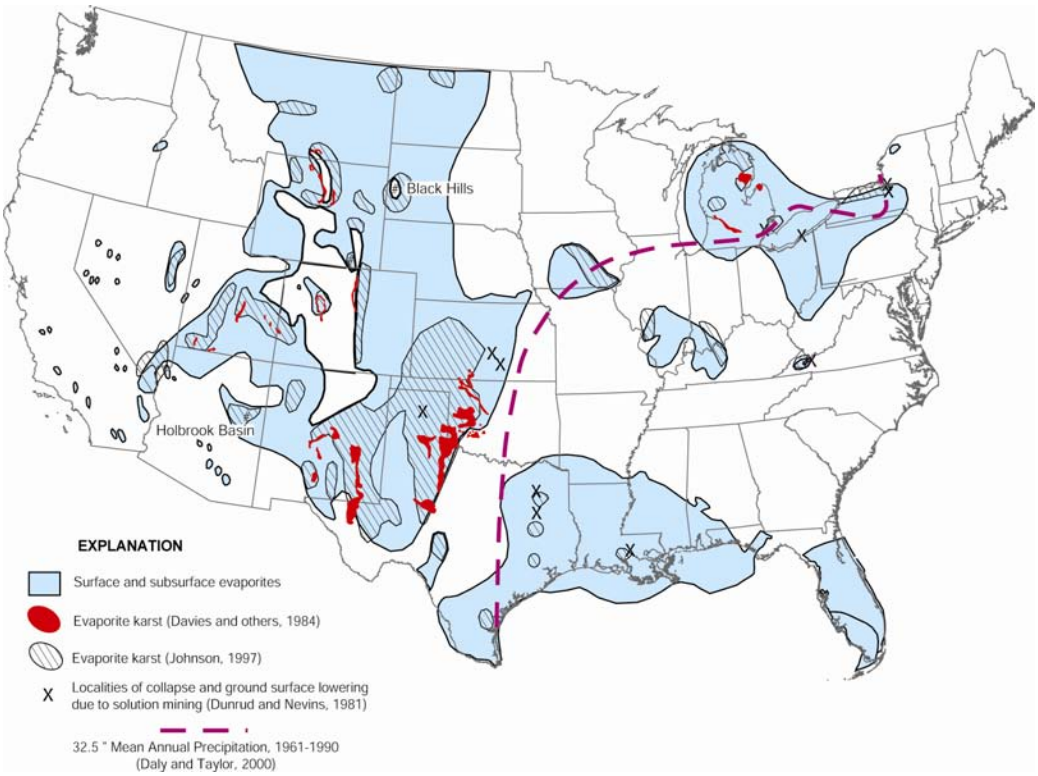

Figure 2. Distribution of outcropping and subsurface evaporite rocks in the United States and areas of reported evaporite karst (from Epstein and Johnson, 2003). The 32.5" mean-annual-precipitation line approximates a diffuse boundary between eastern and western karst.

The Holbrook Basin in east-central Arizona demonstrates that dissolution of deeply buried evaporites can cause subsidence of overlying non-soluble rocks. The basin is more than 100 miles wide and contains an aggregate of about 1,000 feet of salt, anhydrite, and sylvite interbedded with clastic red beds in the Permian Sedona Group (formerly the Supai Group) (Peirce and Gerrard, 1966; Neal and others, 1998; Rauzi, 2000). The top of the salt is between 600 and 2,500 ft below the surface (Mytton, 1973). These workers describe the removal of evaporites at depth along a northwest-migrating dissolution front, causing the development of presently active collapse structures in the overlying Coconino Sandstone and Moenkopi Formation.

For example, in the area about 10 mi northwest of Snowflake, AZ, the Coconino and other rocks dip monoclinally southward along the Holbrook anticline towards a large depression enclosing a dry lake. The depression is the result of subsidence due to evaporite removal. Collapse extends upwards from the salt, forming a network of spectacular sinkholes in the overlying Coconino Sandstone (fig. 4, 5*A*) (Neal and others, 1998; Harris, 2002). Draping of the Coconino has caused opening of extensive tension fissures, some of which are many tens of feet deep (Neal and others, 1998; Harris, 2002) (Fig. 5*B*). If the definition of "karst" is allowed to include subsidence structures due to the dissolution and removal of soluble rocks below and extending upwards into non-soluble rocks, then a separate map category may be needed to delineate these rocks. Thus, any karst map must show non-soluble rocks whose collapse structures are the result of dissolution of evaporite rocks below. A somewhat similar situation prevails in the Black Hills of South Dakota and Wyoming and was alluded to at Stops 3 and 4 of the Southern Field Trip (Epstein, Agenbroad, and others, this volume, 2005).

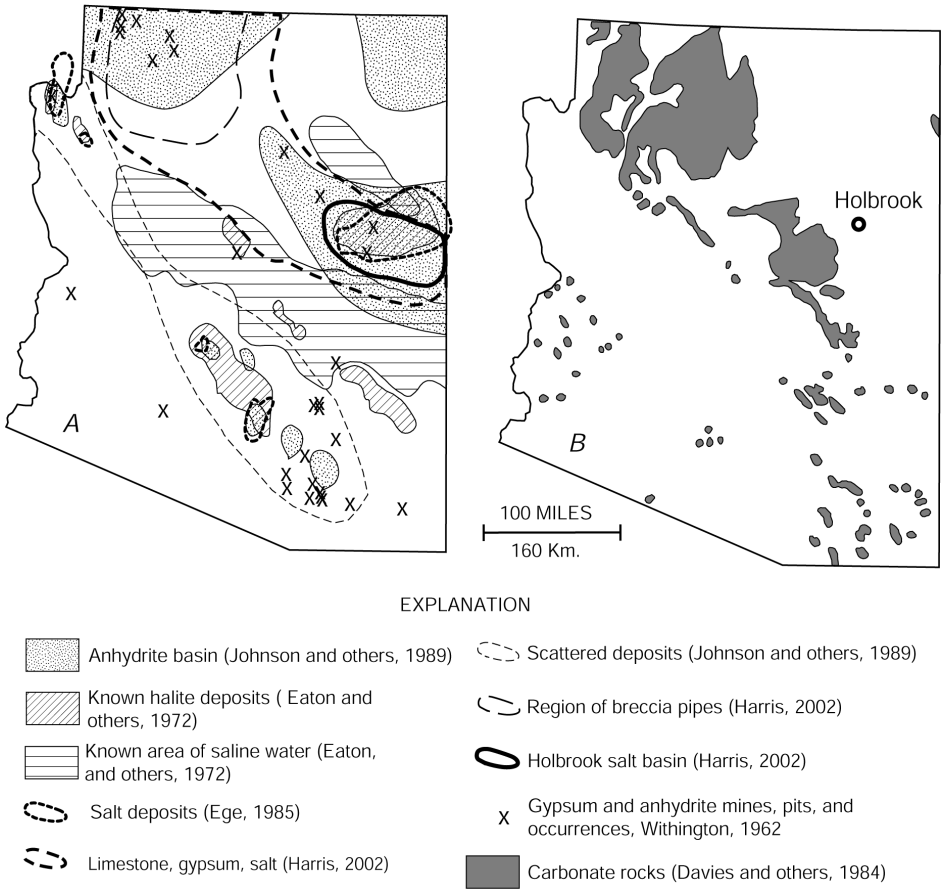

Figure 3. Maps comparing types and distribution of karst features in Arizona: A) distribution of evaporite and carbonate karst as presented by various authors; B) distribution of carbonate karst (no evaporite karst was shown) as presented by Davies and others (1984).

BLACK HILLS, WYOMING AND SOUTH DAKOTA

In the semi-arid Black Hills of Wyoming and South Dakota, significant deposits of gypsum and lesser anhydrite are exposed at the surface in several stratigraphic units (Table 1, Epstein and Putnam, *this volume*), including the Minnelusa, Spearfish, and Gypsum Spring Formations. The field guides that accompany this volume document many of the karst features found in these rocks. The outcrop pattern of sedimentary units in the Black Hills is controlled by erosion on an irregular domal uplift about 130 mi long and 60 mi wide. The central core of Precambrian rock is surrounded by four zones of sedimentary rock with contrasting lithologies and differing karst features. These are, from the center (oldest) outwards: (1) The limestone plateau, made up of Cambrian to Pennsylvanian limestone, dolomite, and silici-clastic rocks, and containing world-class caves such as Wind and Jewel Caves in the Pahasapa Limestone. Overlying these limestones is the Minnelusa Formation, which contains as much as 235 ft of anhydrite in its upper half in the subsurface. This anhydrite has been dissolved at depth, producing a variety of dissolution structures (Stop 1, Epstein, Agenbroad, and others, *this volume;* and Stop 4, Epstein, *this volume*). (2) The Red Valley, predominantly underlain by red beds of the Spearfish Formation of Triassic and Permian age and containing several gypsum beds totaling more than 75 ft thick in places. Dissolution of these evaporites, and those in underlying rocks, has produced shallow depressions and sinkholes, some of which are more than 50 ft deep (Stops 8 and 9, of Epstein, Davis, and others, 2005, this volume). The Gypsum Spring Formation, which overlies the Spearfish, contains a gypsum unit, as much as

15 feet thick, that has developed abundant sinkholes in places. (3) The "Dakota" hogback, held up by resistant Sandstone of the Inyan Kara Group of Cretaceous age, and underlain by shales and sandstones of the Sundance and Morrison Formations. Collapse structures, such as breccia pipes and sinkholes, extend up through some of these rocks from underlying soluble rocks, probably in the Minnelusa Formation. (4) Impure limestone and shale extending outward beyond the hogback, some of which are shown as karstic units on the map of Davies and others (1984), but such features are unknown in those rocks.

Figure 6 compares the map of limestone outcrops shown by Davies and others (1984) for the Black Hills of South Dakota with the more detailed categories that are proposed here, including carbonate and evaporite karst, intrastratal karst, and nonsoluble rocks with collapse features due to dissolution of other rock units at depth. This characterization may also be suitable for other areas of the western United States.

Anhydrite in the Minnelusa is generally not seen in surface outcrops. It has been, and continues to be, dissolved at depth, forming collapse breccias, breccia pipes, and sinkholes that extend upwards more than 1,000 ft into overlying units. Mapping this intrastratal karst is fairly easy, because the outcrop distribution of the Minnelusa is well known. At depth, brecciation of the upper part of the Minnelusa has developed significant porosity, resulting in an important aquifer. Ground water migrates along breccia pipes that extend upwards through overlying formations. A migrating dissolution front (Epstein, 2001; 2003) similar to the situation reported for the Holbrook Basin in Arizona, is summarized below.

Dissolution Front in the Minnelusa Formation

The upper half of the Minnelusa Formation contains abundant anhydrite in the subsurface, and except for a few areas near Beulah and Sundance, Wyoming (Brady, 1931), and in Hell Canyon in the southwestern Black Hills (Braddock, 1963), no anhydrite or gypsum crops out. A log of the upper part of the Minnelusa from Hell Canyon contains 235 ft (72 m) of anhydrite and gypsum (Braddock, 1963; Brobst and Epstein, 1963). Where anhydrite is present in the Minnelusa, its rocks are not brecciated or only slightly so. Where the rocks are brecciated in outcrop, anhydrite is absent. Clearly, the brecciation is the result of collapse following subsurface dissolution of anhydrite.

The Madison and Minnelusa are the major aquifers in the Black Hills. They are recharged by rainfall on and by streams flowing across their up-dip outcrop area. In the Minnelusa, removal of anhydrite progresses downdip with continued dissolution of the anhydrite (fig. 7), collapse breccia is formed, breccia pipes extend upwards, and resurgent springs develop at the sites of sinkholes. Cox Lake, Mud Lake, Mirror Lake, and McNenny Springs (Stop 8, Epstein, Davis, and others, *this volume*), are near the position of the dissolution front. As the Black Hills is slowly lowered by erosion, the anhydrite dissolution front in the subsurface Minnelusa moves downdip and radially away from the center of the uplift. The resurgent springs will dry up and new ones will form down dip as the geomorphology of the Black Hills evolves. Abandoned sinkholes on canyon walls (see figure 8, Epstein, Davis, and others, *this volume*) attest to the former position of the dissolution front.

Because ground water has dissolved the anhydrite in the Minnelusa in most areas of exposure, and because anhydrite is present in the subsurface, a transition zone should be present where dissolution of anhydrite is currently taking place. A model of this zone has been presented by Brobst and Epstein (1963, p. 335) and Gott and others (1974, p. 45) and is shown here in figure 7. Consequences of this model include (1) the up-dip part of the Minnelusa is thinner than the downdip part because of removal of significant thickness of anhydrite, (2) the upper part of the Minnelusa should be continually collapsing, even today, and (3) the properties of the water in this transition zone may be different than elsewhere.

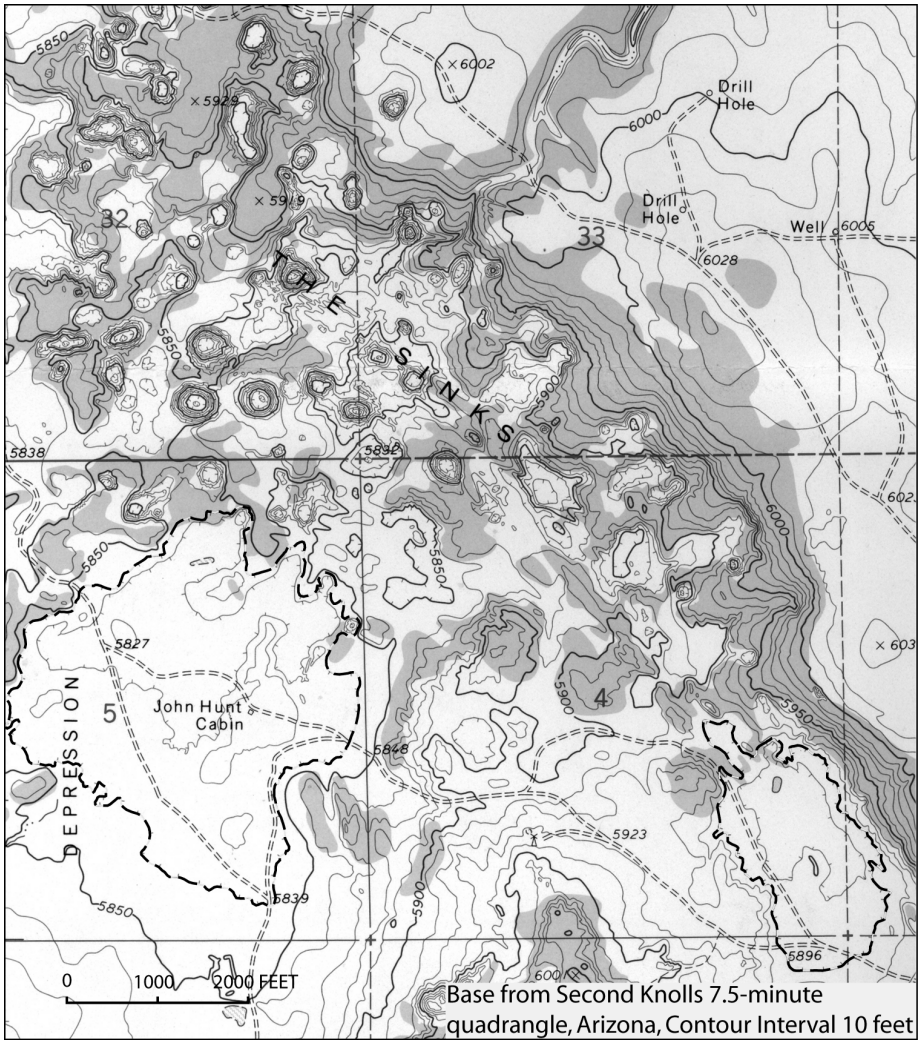

Figure 4. Topographic map of "The Sinks", a series of depressions in the Coconino Sandstone, about 10 miles northwest of Snowflake, Arizona, in the Holbrook basin. Wide depressions are highlighted with a dashed line; the one in the southwest corner of the map is about one mile long. Other depressions are as much as 100 feet deep.

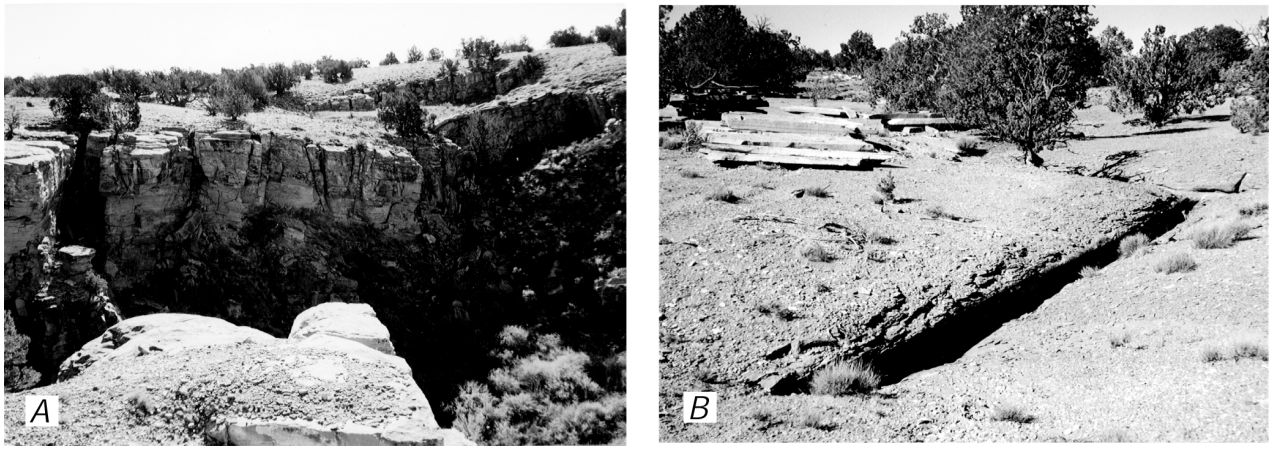

Figure 5. Collapse structures in clastic rocks overlying the salt-bearing Sedona Group in the Holbrook Basin, 8-10 mi northwest of Snowflake, AZ. A) Steep-sided sinkhole in a hole-pocked area called "The Sinks," located in the Coconino Sandstone. Note the variable amount of subsidence along major joints. B) Open tension fractures in the Moekopi Formation caused by flexure of the Holbrook "anticline" (actually a monocline) due to dissolution of salt at depth. Also see figures in Harris (2002).

If this process is correct, then present resurgent springs should be eventually abandoned and new springs should develop down the regional hydraulic gradient of the Black Hills. One example might be along Crow Creek where a cloud of sediment from an upwelling spring lies 1,000 ft (300 m) north of McNenny Springs (See figure 15, Stop 8, Northern Field trip Guide). This circular area, about 200 ft across, might eventually replace McNenny Springs.

Age of Brecciation

Solution of anhydrite in the Minnelusa probably began soon after the Black Hills was uplifted in the early Tertiary and continues today. Recent subsidence is evidenced by sinkholes opening up within the last 20 years (See figure 26, Epstein, Davis and others, this volume), collapse in water wells and natural springs resulting in sediment disruption and contamination, fresh circular scarps surrounding shallow depressions, and calcium sulphate and sodium chloride issuing from spring water throughout the Black Hills.

The brecciation of the upper part of the Minnelusa formation occurred after the up-dip portion of the Minnelusa was breached following uplift. Ground water was then able to penetrate the impermeable layers overlying the Minnelusa and the anhydrite was dissolved. Darton and Paige (1925) found "older terrace deposits" with Oligocene fossils on the Minnelusa, indicating that the breaching of the Minnelusa occurred before the Oligocene and after the Late Cretaceous uplift.

An earlier alternative explanation for the cause and timing of brecciation was given by Bates (1955) who believed the brecciation occurred almost concurrently with the deposition of the Minnelusa when ground water converted the anhydrite to gypsum and the resulting expansion heaved and shattered the surrounding strata leaving jumbled blocks that were reworked by the sea. However, field evidence supports the conclusion that brecciation occurred after, not during, the deposition of the Minnelusa. Disruption of bedding in the Minnelusa and in higher stratigraphic units becomes less intense upwards from the zone of anhydrite removal in the Minnelusa (Stop 1, Epstein, Agenbroad, and others, 2005, *this volume*). Subsidence effects in the overlying formations also become less dramatic. The resistant, thin, Minnekahta Limestone, lying between the red beds of the Opeche Shale and Spearfish Formation, contains few collapse features; some sinkholes penetrate the entire thickness of the Minnekahta and are therefore result of collapse from below (Stop 3, Epstein, Davis, and others, *this volume*). The most significant effect on the Minnekahta is the undulations seen in outcrop everywhere in the Black Hills. Breccia pipes and sinkholes are known as high as the Lakota Formation, about 1,000 feet above the Minnelusa.

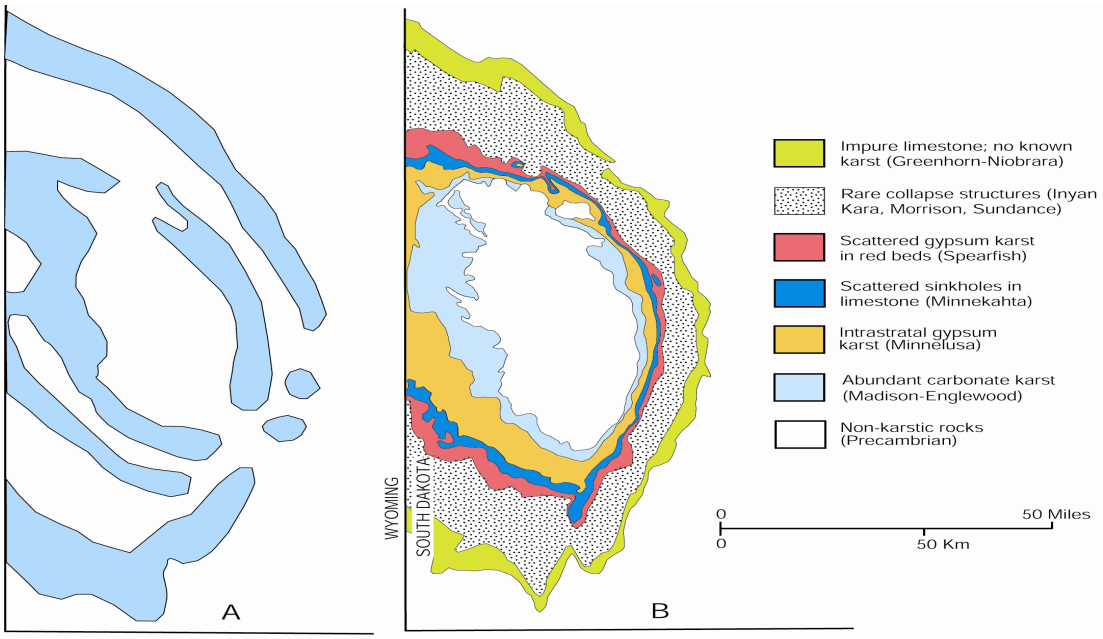

Figure 6. Maps comparing depiction of karst areas in the Black Hills of South Dakota: A) carbonate-karst units, as presented by Davies and others (1984); B) carbonate- and evaporite-karst units, as herein proposed for a new national karst map.

There are several places in the Black hills where bedding in the Minnelusa is moderately or steeply dipping and intruded by breccia pipes. If the pipes formed soon after deposition of Minnelusa sediments, they should be nearly right angles to bedding. Such is not the case, as seen at mileage 59.3 in the Southern Field trip Guide, where the dip of bedding is moderate and shown in figure 8 where the dip is steeper.

HUMID VERSUS SEMI-ARID KARST

Comparing the known locations of surface evaporite karst with a map showing annual average rainfall shows a striking relationship between precipitation and the occurrence of evaporite karst (fig. 2). Most occurrences of surficial karst in gypsum shown in figure 2 lies west of a zone with annual precipitation of about 32 inches (represented by the 32.5-inch isobar). Many of the karst areas shown in figure 2 are due to dissolution at depth. In Michigan, earlier studies suggest that the karstic collapse features there were formed soon after deposition of the Devonian evaporites (Landes, 1945), but Black (1997) showed that sinkhole development occurred after the most recent glaciation.

The degree to which soluble rocks are dissolved depends, in part, on the amount of rainfall and the solubility of the rock. Sulphate-bearing rocks--gypsum and anhydrite--are perhaps 10-30 times more soluble in water than carbonate rocks (Klimchouk, 1996). Both carbonates and sulphates behave differently in the humid eastern United States and the semi-arid to arid west. Low ground-water tables and decreased ground-water circulation in the west does not favor rapid carbonate dissolution and development of karst. In contrast, sulphate rocks are dissolved much more readily and actively than carbonate rocks, even under semi-arid to arid conditions. The presence of extensive karst in carbonates in the west probably dates to a more humid history. Additionally, the generally thicker soils in humid climates provide the carbonic acid that enhances carbonate dissolution. Gypsum and anhydrite, in contrast, are more readily soluble in water that lacks organic acids. This relationship suggests an interesting area for future study.

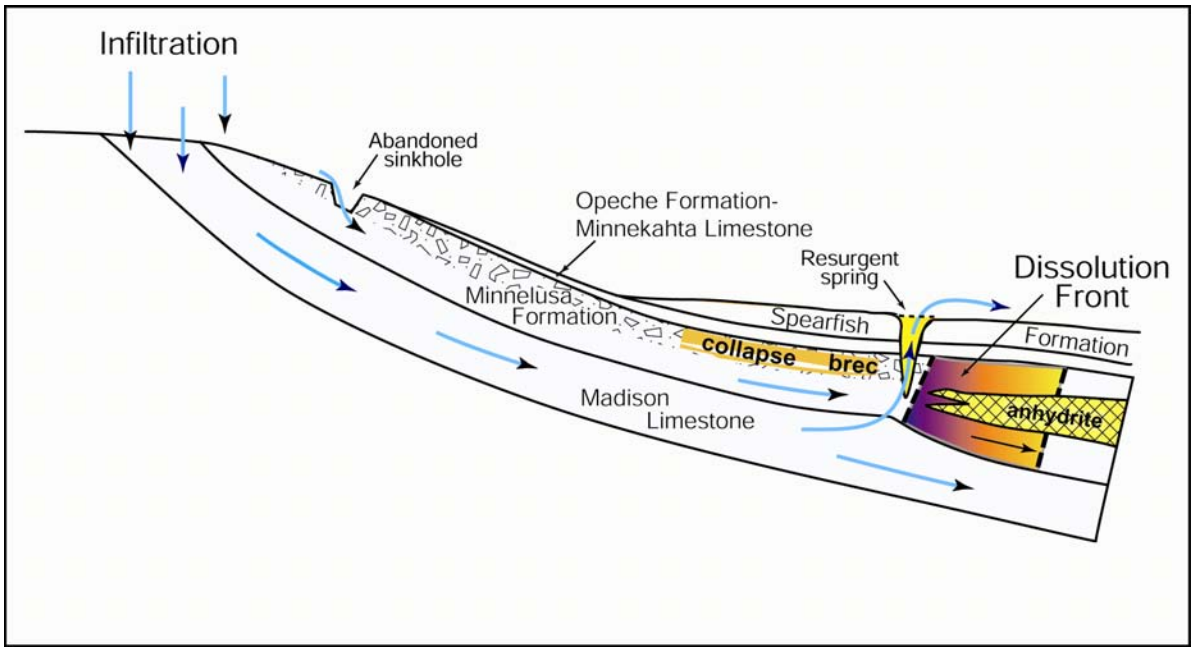

Figure 7. Dissolution of anhydrite in the Minnelusa Formation and down-dip migration of the dissolution front.

In the eastern United States karstification occurs by acid-charged water percolating *downward*, altering soluble rocks below. While this is partly true in the west, much of the karst, such as in the Black Hills, is produced by artesian water migrating *upward*, affecting overlying rocks in a different manner than in the humid east. Thus, as shown above, non-soluble rocks bear the imprint of karst.

HUMAN-INDUCED KARST

It is well known that subsidence in karstic rocks can be exacerbated by human activities. Lowering of the water table by well-pumping or by draining of quarries can reduce support of soils overlying sinkholes, thus causing their collapse. Subsurface mining of salt and other evaporites may eventually cause collapse of overlying rocks, such as at the Retsof mine in Livingston County, NY (Nieto and Young, 1998; Gowan and Trader, 2003). Localities of subsidence due to solution mining were mapped by Dunrud and Nevins (1981) and are shown in figure 2. The bibliographic list of ground subsidence due to evaporite dissolution of Ege (1979) contains many instances where such subsidence was due to human activities. Knowing the location of shallow and deep mines is important to local officials, in order to understand the potential for such subsidence. For example, abandoned gypsum mines in western New York are abundant, and recent settlement of many houses near Buffalo, New York, partly may be the result of subsidence over these mines.

Figure 8. Near-vertical breccia pipe (short dash) in steeply dipping beds (long dash) of the Minnelusa Formation, Frannie Peak Canyon, Fanny Peak 7.5-minute Quadrangle, six miles southeast of Newcastle, Wyoming, NW1/4 SE1/4, T. 44 N., R. 60 W.

REFERENCES

Bates, R. L., 1955, Permo-Pennsylvanian formations between Laramie Mountains, Wyoming, and Black Hills, South Dakota: Am. Assoc. Petroleum Geologists Bull., v. 39, p. 1979-2002.

Black, T.J., 1997, Evaporite karst of northern lower Michigan: Carbonates and Evaporites, v. 12, p. 81-83.

Braddock, W.A., 1963, Geology of the Jewel Cave SW Quadrangle, Custer County, South Dakota: U.S. Geological Survey Bulletin 1063-G, p. 217-268.

Brady, F. H., 1931, Minnelusa formation of Beulah district, northwestern Black Hills, Wyoming: Am. Assoc. Petroleum Geologists Bull., v. 15, p. 183-188

Brobst, D.A., and Epstein, J.B., 1963, Geology of the Fanny Peak quadrangle, Wyoming-South Dakota: U.S. Geological Survey Bulletin 1063-I, p. 323-377.

Daly, Chris, and Taylor, George, 2000, United States Average Annual Precipitation, 1961-1990: Spatial Climate Analysis Service, Oregon State University; USDA -NRCS National Water and Climate Center, Portland, Oregon; USDA -NRCS National Cartography and Geospatial Center, Fort Worth, Texas; Online linkage: <http:/ /www.ftw.nrcs.usda.gov/prism/prism-data.html>

Darton, N.H., and Paige, Sidney, 1925, Description of the central Black Hills, South Dakota: U.S. Geological Survey Geologic Atlas, folio 219, 34 p.

Davies, W.E., Simpson, J.H., Ohlmacher, G.C., Kirk, W.S., and Newton, E.G., 1984, Map showing engineering aspects of karst in the United States: Reston, Va., U.S. Geological Survey National Atlas of the United States of America, scale 1:7,500,000.

Dunrud, C.R., and Nevins, B.B., 1981, Solution mining and subsidence in evaporite rocks in the United States: U.S. Geological Survey Miscellaneous Investigation Series Map I-1298, 2 sheets.

Eaton, G.P., Peterson, D.L., and Schumann, H.H., 1972, Geophysical, geohydrological, and geochemical reconnaissance of the Luke salt body, central Arizona: U.S. Geological Survey Professional Paper 753, 28 p.

Ege, J.R., 1979, Selected bibliography on ground subsidence caused by dissolution and removal of salt and other soluble evaporites: U.S. Geological Survey Open-file Report 79-1133, 28 p.

Ege, J.R., 1985, Maps showing distribution, thickness, and depth to salt deposits of the United States: U.S. Geological Survey Open-File Report 85-28, 11 p.

Epstein, J.B., 2001, Hydrology, hazards, and geomorphic development of gypsum karst in the northern Black Hills, South Dakota and Wyoming: U.S. Geological Survey, report WRI 01-4011, p. 30-37.

Epstein, J.B., 2003, Gypsum karst in the Black Hills, South Dakota-Wyoming; Geomorphic development, hazards, and hydrology: Oklahoma Geological Survey, report 109, p. 241-254.

Epstein, J.B., 2005, Field Trip Guide 3, Karst Field Trip to the Western Black Hills: *in*, Kuniansky, E.L., editor, U.S. Geological Survey, Karst Interest Group Proceedings, Rapid City, South Dakota, September 12-15, 2005, this volume: U.S. Geological Survey Scientific Investigations Report Series 2005-5160, this volume.

Epstein, J.B., Agenbroad, Larry, Fahrenbach, Mark, Horrocks, R.D., Long, A.J., Putnam, L.D., Sawyer, J.F., and Thompson, K.M., 2005, Field Trip Guide 1, Karst Field Trip to the Southern Black Hills: *in*, Kuniansky, E.L., editor, U.S. Geological Survey, Karst Interest Group Proceedings, Rapid City, South Dakota, September 12-15, 2005, this volume: U.S. Geological Survey Scientific Investigations Report Series 2005-5160, this volume.

Epstein, J.B., Davis, A.D., Long, A.J., Putnam, L.D., and Sawyer, J.F., 2005, Field Trip Guide 2, Karst Field Trip to the Northern Black Hills: *in*, Kuniansky, E.L., editor, U.S. Geological Survey, Karst Interest Group Proceedings, Rapid City, South Dakota, September 12-15, 2005, this volume: : U.S. Geological Survey Scientific Investigations Report Series 2005-5160, this volume.

Epstein, J.B., and Putnam, L.D., 2005, Introduction to three field trip guides: karst features in the Black Hills, Wyoming and South Dakota—Prepared for the Karst Interest Group Workshop, September 2005: *in*, Kuniansky, E.L., editor, U.S. Geological Survey, Karst Interest Group Proceedings, Rapid City, South Dakota, September 12-15, 2005, this volume: U.S. Geological Survey Scientific Investigations Report Series 2005-5160, this volume.

Epstein, J.B., and Johnson, K.S., 2003, The need for a national evaporite-karst map, *in*, Johnson, K.S., and Neal, J.T., eds, Evaporite karst and engineering/environmental problems in the United States: Oklahoma Geological Survey Circular 109, p. 21-30.

Gott, G.B., Wolcott, D.E., and Bowles, C.G., 1974, Stratigraphy of the Inyan Kara Group and localization of uranium deposits, southern Black Hills, South Dakota and Wyoming: U.S. Geological Survey Professional Paper 763, 57 p.

Gowan, S. W., and Trader, S. M., 2003, Mechanism of Sinkhole Formation in Glacial Sediments above the Retsof Salt Mine, Western New York *in*, Johnson, K.S., and Neal, J.T., eds, Evaporite karst and engineering/environmental problems in the United States: Oklahoma Geological Survey Circular 109, p. 21-30.

Harris, R.C., 2002, A review and bibliography of karst features of the Colorado Plateau, Arizona: Arizona Geological Survey, Open-File Report 02-07, 43p.

Johnson, K.S., 1997, Evaporite karst in the United States: Carbonates and Evaporites, v. 12, p. 2-14.

Johnson, K.S., and Gonzales, S., 1978, Salt deposits in the United States and regional geologic characteristics important for storage of radioactive waste; Prepared for Union Carbide Corporation, Nuclear Division, Office of Water Isolation, Y/OWI/SUB-7414/1, 188 p.

Johnson, K. S., Gonzales, S., and Dean, W. E, 1989, Distribution and geologic characteristics of anhydrite deposits in the United States, *in* Dean, W.E.; and Johnson, K.S. (eds.), Anhydrite deposits of the United States and characteristics of anhydrite important for storage of radioactive wastes: U.S. Geological Survey Professional Paper 1794, p. 9–90.

Klimchouk, Alexander, 1996, The dissolution and conversion of gypsum and anhydrite, *in* Klimchouk, Alexander; Lowe, David; Cooper, Anthony; and Sauro, Ugo (eds.), Gypsum karst of the World: International Journal of Speleology, v. 25, nos. 3-4, p. 21-36.

Landes, K.K., 1945, The Mackinac Breccia: Michigan Geological Survey Publication 44, p.121-154.

Laury, R.L., 1980, Paleoenvironment of a late Quaternary mammoth-bearing sinkhole deposit, Hot Springs, South Dakota: Geological Society of America Bulletin, v. 91, p. 465-475

Mytton, J. W., 1973, Two salt structures in Arizona--the Supai salt basin and the Luke salt body: U.S. Geological Survey Open-file report, 40 p.

Nieto, A.S., and Young, R. A., 1998, Retsof salt mine collapse and aquifer dewatering, Genesee Valley, Livingston County, New York, *in* Borchers, J. W. (ed.), Land subsidence case studies and current research; Proceedings of the Dr. Joseph F. Poland Symposium on Land

Subsidence: Association of Engineering Geologists Special Publication 8, p. 309-325.

Neal, J.T., Colpitts, R., and Johnson, K.S., 1998, Evaporite karst in the Holbrook Basin, Arizona: *in*, Borchers, J.W., ed., Land subsidence case studies and current research: Proceedings of the Dr. Joseph F. Poland Symposium on Land Subsidence: Association of Engineering Geologists Special Publication No. 8, p. 373-384.

Peirce, H. W., and Gerrard, T. A., 1966, Evaporite deposits of the Permian Holbrook basin, Arizona, *in* Rau, J. L., ed., Second symposium on salt, 1973: Cleveland, Ohio, Northern Ohio Geological Society, v. 1, p. 1-10.

Rauzi, S. L., 2000, Permian salt in the Holbrook Basin, Arizona: Arizona Geological Survey, Open-File Report 00-03, 20 p.

Withington, C. F., 1962, Gypsum and anhydrite in the United States, exclusive of Alaska and Hawaii: U.S. Geological Survey Mineral Investigations Resource Map MR-33.

Gypsum and Carbonate Karst Along the I-90 Development Corridor, Black Hills, South Dakota

By Larry D. Stetler and Arden D. Davis
Department of Geology and Geological Engineering, South Dakota School of Mines and Technology, Rapid City, South Dakota 57701

ABSTRACT

The Interstate 90 development corridor extends from Rapid City to Spearfish, South Dakota, and overlies several formations that exhibit gypsum and carbonate karst features. Karst development commonly occurs within sections of three formations in the Black Hills region. The oldest karst features occur in the Mississippian Madison Limestone, a limestone-dolomite system that exhibits a karsted surface as well as extensive cave formation. The Pennsylvanian-Permian Minnelusa Formation contains anhydrite and thin limestone beds that have undergone localized and varied karstification. Hydration and swelling of primary anhydrite has resulted in multiple collapse structures within the formation. The Triassic Spearfish Formation contains gypsum deposits throughout; however, massively bedded gypsum up to 10 m thick is contained at the top in the Gypsum Spring Member.

All of these formations can exhibit karst topography and features where exposed, but their properties also influence ground-water flow in the subsurface. Dye tracer tests and geochemical analyses have provided evidence that flow paths through these formations are controlled largely by karst features and associated fracture systems. Ground water in the Madison aquifer in the Rapid City area converges from flows through karst from different surface watersheds to the south and the north. Springs at or near the contact of the Permian Minnekahta Limestone and the overlying Spearfish Formation have been chemically tied to Madison water, indicating upward flow through collapse breccia in both the Minnelusa and Spearfish formations. In addition, sinkholes are common occurrences in the Spearfish Formation throughout the Interstate 90 development corridor in the Black Hills.

Ground water supplies much of the municipal and private water needs in the Black Hills. As development continues throughout the region, ground-water protection should receive focused attention, particularly along the I-90 development corridor. Current research is aimed toward geologic mapping, hazard identification, and assessment as tools to inform the general public and as planning guides for local governments.

Karst Features as Animal Traps: Approximately 500,000 Years of Pleistocene and Holocene Fauna and Paleoenvironmental Data from the Northern High Plains

By Larry D. Agenbroad and Kristine M. Thompson
Mammoth Site of Hot Springs, South Dakota, Inc., P. O. Box 692, Hot Springs, SD 57747

ABSTRACT

Karst sinkhole features have served as natural animal traps for at least 500,000 years in the uplifted regions of the northern High Plains. We examine reported karst traps that have faunas ranging from greater than 451,000 years ago, upward through Holocene time. Chronologies are based on tephra, biostratigraphy, and absolute dating. Full glacial and interglacial faunas from the late Irvingtonian Land Mammal Age through the Rancholabrean Land Mammal Age into the Holocene, are represented. As such, sinkhole traps serve as time capsules preserving extinct fauna and clues to past environments.

INTRODUCTION

Fossil vertebrates dating to the mid-Pleistocene (Irvingtonian Land Mammal Age) to Holocene are known from filled and partially filled karst features. Located in the uplifted areas of the northern High Plains (Figure 1), at least seven of these features have served as natural traps yielding faunal and paleoenvironmental data covering the last 500,000 years. These repositories are often bell shaped solution caverns with narrow openings, allowing ingress, but preventing egress for trapped fauna. Some of the features have filled with talus, roof collapse and both eolian and alluvial sediments. Others have been sealed off naturally and have only recently been reopened. One natural trap (the Mammoth Site of Hot Springs, South Dakota) is a former karst feature preserved by differential erosion, creating a topographic high from a former topographic low (sink).

All these karst traps have one thing in common- they are the result of dissolution of limestone or dolomite, and possibly even gypsum. Often the opening to the cave is very small, sometimes only a slot due to dissolution along fractures in the crystalline rocks. Others are the result of roof collapse creating small, somewhat circular openings. Still others represent massive cavern roof collapse creating breccia pipes extending to the surface. At least one karst trap (the Vore Buffalo Jump) is postulated to be the result of solution of gypsum beds within the Spearfish Formation (Epstein 2005).

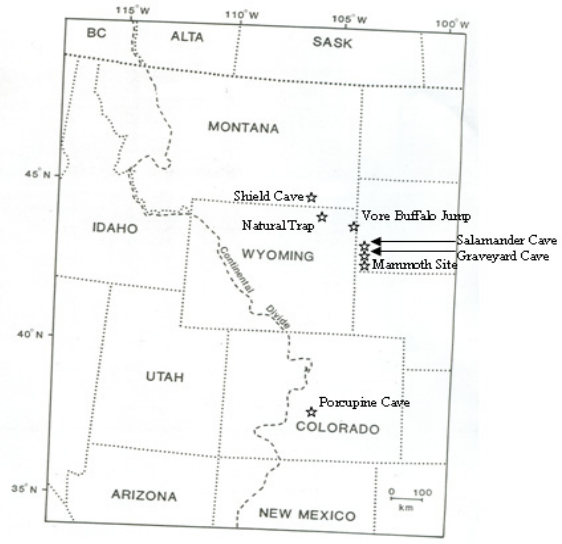

Figure 1. Locality of Karst natural animal traps.

Figure 1. Locality of karst and natural animal traps.

Many of these traps are located on, or near, the tops of ridges (Natural Trap, Salamander Cave, Graveyard Cave, Shield Cave) which were animal trails, especially during periods of heavy snow accumulation. As such, with small entrance openings, they may have been masked by drifting snow, concealing the entrance to the trap. Some features, such as Natural Trap, Wyoming, maintained a snow cone on top of the talus and debris, allowing for lateral dispersal of large, heavy bodied fauna.

DESCRIPTIONS

Middle to late Pleistocene

Natural Trap, Wyoming

This trap is a large, somewhat bell-shaped cavern formed in the Madison Formation of Mississippian age (Figures 1, 2a, and 3; Table 1). The entrance is small with a free fall of up to 85 ft (27 m) as illustrated in Fig. 2. The entrance is located on a ridge which serves as a major animal trail from the summit of the Bighorn Mountains to the valley floor of the Bighorn River. The entrance is small enough to be hidden almost until at the edge, and it served as a trap for pursued herbivores and their pursuing carnivores.

Excavation has only proceeded to a depth of about 25 ft (8 m), ceasing at a volcanic ash dating to 110,000 years ago. There are still bones beneath this marker horizon, but they have yet to be investigated. Several extinct, late Pleistocene megafauna (animals over 100 pounds live weight) are represented, including mammoth, horses, musk oxen, American lions, short-faced bears, and other mammals. The first record of the cheetah in North America comes from this cave. Most of the studied fauna occur in the 12,000 to 20,000 year old horizons (Martin and Gilbert, 1978; Gilbert and Martin, 1984).

Botanical information records a C-3 grassland being replaced by a C-4 grassland at around 12,000 years ago. A paleoenvironmental interpretation is that of an arctic steppe in a cooler, wetter environment, becoming warmer and drier as it approached the modern conditions. As such, the deposits reflect the last interglacial (Sangomon), the last glacial (Wisconsinan) and Holocene interglacial.

Porcupine Cave, Colorado

Originally formed in an Ordovician age Manitou Dolomite, Porcupine Cave was sealed naturally, in the middle Pleistocene and reopened by miners (Figures 1, 2b, and 3; Table 1). Based on biostratigraphy, (Table 1) the deposits range from approximately 487,000 to 365,000 years ago (Anderson 1996; Barnowski et aI., 1996). The fauna represents a glacial (Illinoian) to interglacial (Sangamonian) environmental change. Significant information on the paleoenviroment of this period had been determined by the rich floral and faunal record.

Salamander Cave, South Dakota

A solution cavern in the Mississippian age Madison Limestone, Salamander Cave has a narrow, slot opening from dissolution along a fracture zone (Figures 1, 2c, and 3; Table 1). The cave has two major chambers and the horse room is a naturally sealed cave with a narrow connection to the modern entrance room. A flowstone seals the bone bearing stratum revealed in a crystal hunters prospect pit. Uranium-Thorium (U/Th) dates on the flowstone are 252,000 years ago (Mead et al. 1996). It is estimated that initial bone deposition could have been as early as 451,000 years ago, based on biostratigraphy and a statistical estimate based on the U/Th dating (Mead et al. 1996). These data suggest a glacial (Illinoian) followed by an interglacial, (Sangamonian) followed by the Wisconsinan glacial, and the Holocene interglacial.

Late Pleistocene to Holocene

Mammoth Site, South Dakota

The Mammoth site is a filled karst feature which served as a conduit for thermal artesian springs, creating a pond within the sinkhole confines (Figures 1, 2d, and 3; Table 1). It became a natural trap, selective for young, male mammoths and their behavior patterns. In addition, 47 species of other fauna were also preserved in this deposit. An average radiocarbon age from one stratigraphic horizon provides a date of 26,000 years ago (Agenbroad 1994). It may have been an active trap for 300 to 750 years, ceasing to trap animals after the downcutting Fall River caused lateral migration of the artesian springs. The deposit is elliptical in form, roughly 150 ft (46 m) by 125 ft (38 m). Drill cores by the South Dakota Geological Survey indicate a depth of greater than 65 ft (22m). Animals attracted to vegetation along the rim of a warm water pond were attracted into the sink, to find they could not climb out due to the wet, slippery, Spearfish Shale, and died of starvation or fatigue. Carnivores were attracted to the deposit by the smell of decaying animals. Some smaller fauna may have been

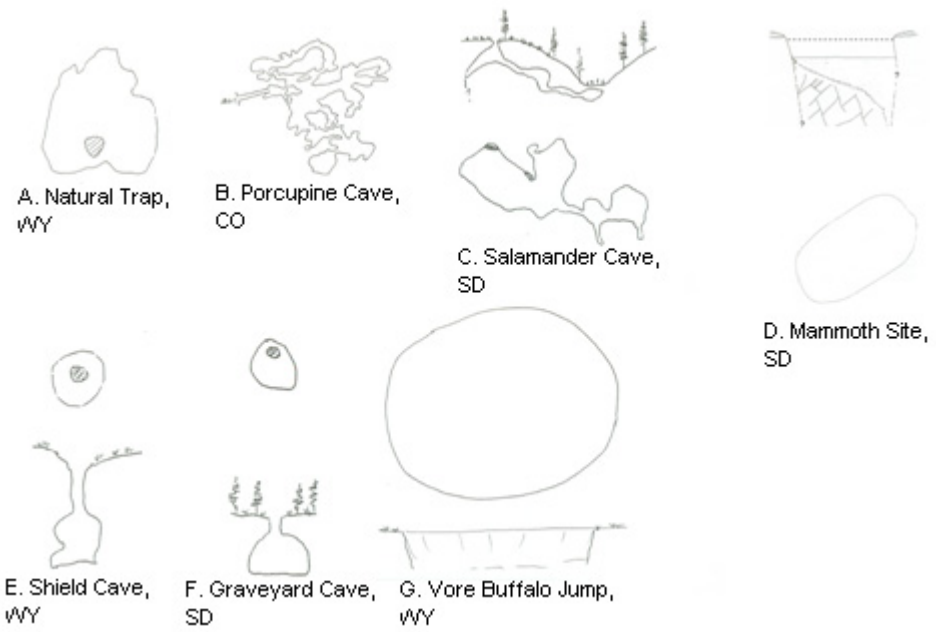

Figure 2.—Plan and profile of karst animal traps in High Plains

Table 1. Generalized faunal assemblages from High Plains Karst traps

[V=Vore site, WY; G=Graveyard Cave, SD; Sa=Salamander Cave, SD; M=Mammoth Site, SD; NT=Natural Trap, WY; Sh=Shield Cave, MT; P=Porcupine Cave, CO]

Non-mammals	V	G	Sa	M	NT	Sh	P
Mollusca		X		X			X
Pisces				X			X
Amphibia		X	X	X			X
Reptilia		X					X
Aves		X		X	X		X
Mammals							
Insectivora		X					X
Chiroptera		X		X			X
Xenarthra							X
Lagomorpha		X	X	X	X	X	X
Rodentia							
Sciuridae		X	X	X	X	X	X
Geomyidae		X		X			X
Heteromyidae		X		X			X
Cricetidae		X	X	X	X		X
Eretezontidae		X	X			X	X
Carnivora							
Mustelidae		X	X	X	X	X	X
Canidae		X	X	X	X	X	X
Felidae				X(?)	X		X
Ursidae				X	X	X	X
Perissodactyla							
Equidae			X		X	X	X
Artiodactyla							
Tayassuidae							X
Camelidae				X	X	X	X
Cervidae		X					X
Antilocapridae			X	X	X		X
Bovidae	X	X			X	X	X
Proboscidea							
Elephantidae				X	X		

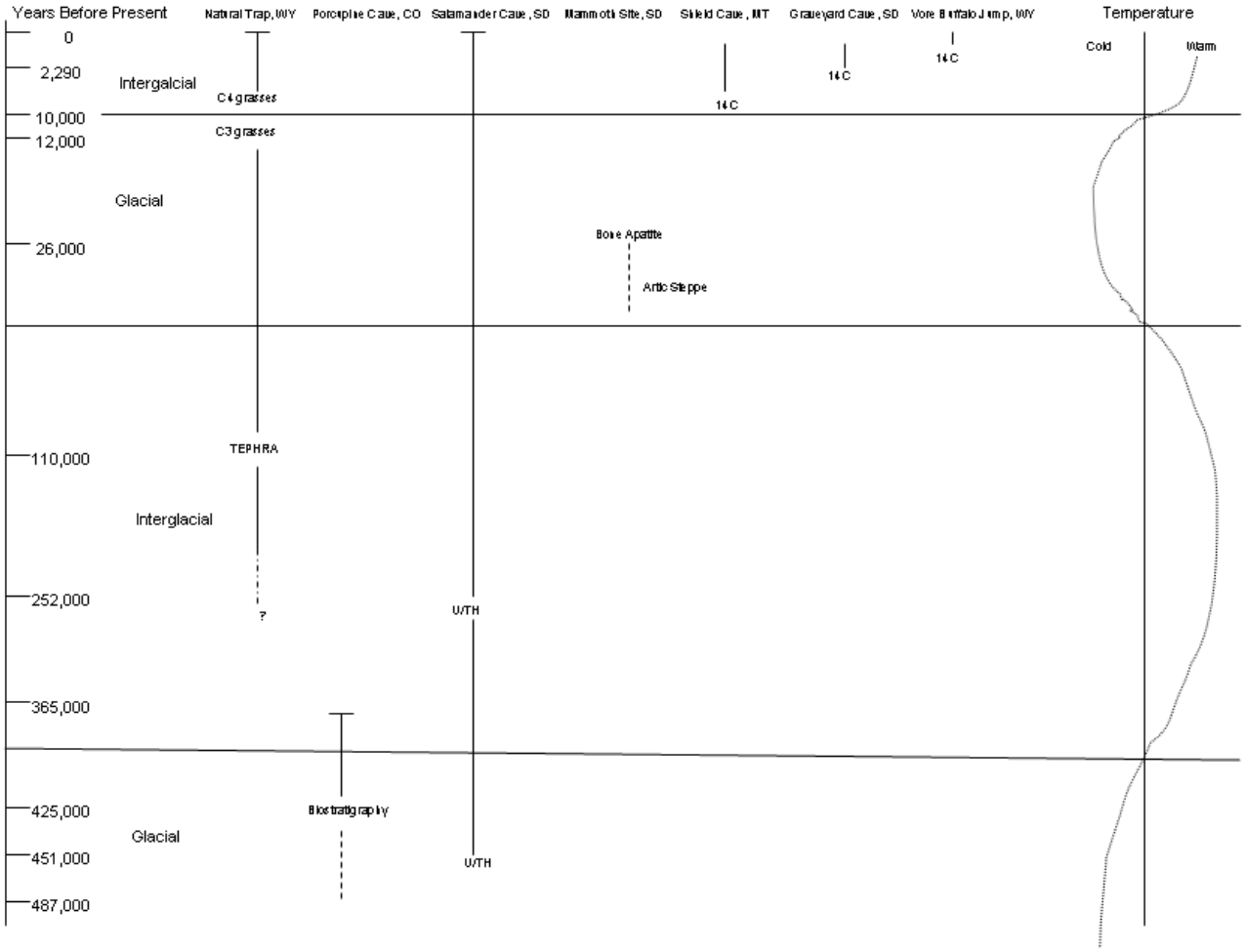

Figure 3.—Chronology and paleoclimate of karst natural animal traps.

incorporated by being washed into the sinkhole from surrounding uplands. The reworked, cemented sediment filling the sinkhole were more resistant to differential erosion, and the former low topographic expression became a modem topographic high.

Shield Cave, Montana

Shield Cave is a 46 ft (14 m) deep bell-shaped cave in the Mississippian age Madison Limestone (Figures 1, 2e, and 3; Table 1). The trap is located near the top of a southwest ridge at an altitude of 6549 ft (2606 m), in the Pryor Mountains in Carbon County, Montana. The floor of the chamber is about 15 ft (5m) wide in an elliptical configuration. The trap collected animals from 9,230 years ago to 1,250 years ago. At least 13 species of fauna have been identified from the site. The prominent fauna represented is bison. Other fauna from the deposits include prairie dogs and grizzly bears (Oliver, 1989).

Graveyard Cave, South Dakota

Graveyard Cave is located in Wind Cave National Park and is a small, bell-shaped pit. There is a small, circular opening along the north wall which allowed entrance for Holocene animals (Figures 1, 2f, and 3; Table 1). The floor of the cave is literally carpeted with bones. Manganaro (1994) investigated a 3 ft by 3 ft square test pit in the southeast floor of the cave. A radiocarbon date of ~~2290 BP~~ indicates a late Holocene accumulation. Thousands of bones were sorted from the fill and one bone awl was identified. The site was described as an archaeological site on the basis of this one anomalous artifact. We suggest it is a paleontological site with one probable artifact.

Vore Buffalo Jump, Wyoming

The Vore Buffalo Jump is an open sinkhole located between the westbound and eastbound lanes of the interstate (1-90), just west of the South Dakota state line near Beulah, Wyoming (Figures 1, 2g, and 3; Table 1). Testing by the University of Wyoming, prior to highway construction, indicates the sinkhole was used, repeatedly, as a buffalo jump for at least 300 years. Plains Indians trapped and slaughtered thousands of bison by stampeding the animals over the steep rim. At least 22 stratified layers of bison bone beds have been recorded in the sinkhole fill. Radiocarbon dates and artifact typology place the period of use for this trap at the middle to late prehistoric interval, about 450 years ago (Frison 1991). Epstein (2001) suggests the sinkhole may have formed by solution of gypsum beds in the lower Spearfish Formation.

CONCLUSIONS

The information provided by the seven karst animal traps in the northern High Plains is presented here. Nearly 500,000 years of faunal and environmental data are represented in the interval represented in these deposits. At least the last two glacial and interglacial intervals are represented by both faunal and more limited botanical interpretations. The presence of highly fractured and tilted carbonates in the uplifted areas of this physiographic region provide the possibility of many more solution features than have currently been investigated, or reported. This information indicates the high potential of additional time capsules recording both extinct and extra local faunal assemblages, and the prospect of additional paleoenvironmental data.

REFERENCES CITED

Anderson, E. 1996, A preliminary report on the Carnivora of Porcupine Cave, Park County, Colorado in K. M. Stewart and K. L. Seymour, eds., Palaeoecology and Palaeoenvironment of late Cenozoic mammals, University of Toronto Press, Toronto. p. 259-282.

Barnowsky, A. D., Rouse, T.I., Hadly, E.A., Wood, D.L., Keesing, F.L., and Schmidt, V.A., 1996, Comparison of mammalian response to glacial-interglacial transitions in the middle and late Pleistocene, in K. M. Stewart and K. L.Seymour, eds., Palaeoecology and palaeoevnironment of late Cenozoic mammals. University of Toronto Press, Toronto. p. 16-33.

Epstein, J. B. 2001. Hydrology, hazards and geomorphic development of gypsum karst in the northern Black Hills, South Dakota and Wyoming, in Kuniansky, E.L., ed.,U.S. Geological Survey Karst Interest Group Proceedings, St. Petersburg, Florida February 13-16, 2001, Water-Resources Investigations Report 01-4011, p. 30.37.

Frison, G. C. , 1991, Prehistoric hunters of the High Plains: San Diego, CA, Academic Press, p. 226-229.

Gilbert, B. M. and Martin, L.D.,1984, Late Pleistocene fossils of Natural Trap Cave, Wyoming, and the climatic model of extinction, in P. S. Martin and R. G. Klein eds. Quaternary Extinctions: the search for a cause. University of Arizona Press, Tucson. p. 138-147.

Manganaro, C. A., 1994, Graveyard Cave: a Holocene faunal record from the Black Hillsof South Dakota. Unpublished Master of Science thesis. Northern Arizona University. 119p.

Martin. L. D. and Gilbert, B.M, 1978, Excavations at Natural Trap Cave. Transactions of the Nebraska Academy of Sciences 6:107-116.

Mead, J. 1., Manganaro, C.A., Reppening, C.A. and Agenbroad, L.D., 1996, Early Rancholabrean mammals fromSalamander Cave, Black Hills, South Dakota. in K. M. Stewart and K. L. Seymour eds. Palaeoecology and palaeoenviroment of late Cenozoic mammals. University of Toronto Press, Toronto. p. 458-482.

Oliver, J. S., 1989, Analogues and site context: bone damages from Shield trap Cave (24CB91),Carbon County, Montana, USA. in R. Bonnichsen and M. H. Sorg eds. Bone Modification: Dexter, MT. Thompson-Shore, Inc. p. 73-98.

Developing a Cave Potential Map of Wind Cave to Guide Exploration Efforts

By Rodney D. Horrocks
Wind Cave National Park, RR 1 Box 190, Hot Springs, SD, 57747

ABSTRACT

Although the known boundaries of Wind Cave are expanding only gradually, the length of the overall survey is increasing at a rate of about four miles per year. This expansion reflects the on-going exploration and survey work by cavers. As an aide to these exploration efforts, a cave potential concept was developed. However, the cave potential map actually serves many purposes, including, determining the likely maximum likely potential of the cave, calculating the potential length of the cave survey, identifying likely areas where significant cave may be discovered, determining the relationship, if any, with nearby Jewel Cave, determining the cave watershed boundaries, identifying potential land management partners, and guiding future land management decisions. This paper will focus on the first four purposes related to cave exploration. To develop the cave potential map, several data sets were gathered, including: structural geological factors, a contour map, plan and profile views of the cave survey, radio location data, geology map, blowhole location map, water table contour map, geographic information system (GIS) generated triangular irregular networks (TIN), orthophotoquads, and a park boundary map. By combining these data sets, this exercise demonstrated that is it unlikely that Wind and Jewel Caves are connected, while at the same time it identified the maximum likely potential of Wind Cave. By calculating passage density within the current boundaries of Wind Cave and then for the maximum likely boundaries, a minimum and maximum potential length of the cave was calculated. It was determined that the current cave boundaries cover 1/8 of the total maximum likely potential of the cave. Interestingly, the maximum potential boundaries are roughly 97 percent inside of the current boundaries of Wind Cave National Park. Based on passage density, the length of the Wind Cave survey could range from 400 kilometers (250 miles) to 1,760 kilometers (1,100 miles). The final length depends on whether the boundaries remain as they currently are or if they were expanded to their maximum likely potential. Since the current 185.6 kilometers (116 miles) of survey represents no more than 46 percent of the minimum predicted length of the cave or as little as 10 percent of the maximum predicted length of the cave, it is obvious that a tremendous amount of surveyable passage remains in the system.

The Potential Extent of the Jewel Cave System

By Michael E. Wiles
Jewel Cave National Monument, 11149 US Highway 16, Bldg.12, Custer, SD 57730

ABSTRACT

Currently, over 50 miles (40 percent) of the known cave system is outside park boundaries, and barometric airflow studies indicate that as much as 95 percent remains to be discovered. A first approximation of the maximum extent of humanly passable cave passages based on volume estimates from barometric air flow, constraints presented by geologic contacts, the water table, and known structural features have been modeled. These relationships were quantified and analyzed using structural and potentiometric contours from the U.S. Geological Survey Black Hills Hydrologic Study, surface and subsurface mapping by the National Park Service, and other sources. The model serves as an important management tool for an enormous resource requiring proactive measures to ensure its continued protection.

Geologic Controls on a Transition Between Karst Aquifers at Buffalo National River, Northern Arkansas

By Mark R. Hudson[1], David N. Mott[2], Kenzie J. Turner[1], and Kyle E. Murray[3]
[1] U.S. Geological Survey, Box 25046, MS 980, Denver, CO 80225
[2] National Park Service, Buffalo National River, Harrison, AR 72601
[3] University of Texas at San Antonio, San Antonio, TX 78249

ABSTRACT

Most major springs, in the central part of the 190-km-long Buffalo River watershed of northern Arkansas, discharge from limestone of the Mississippian Boone Formation (the Springfield Plateau aquifer). However, the largest spring, Mitch Hill Spring, discharges from dolostone of the lower part of the underlying Ordovician Everton Formation (part of the Ozark Plateau aquifer). New dye tracer studies and geologic mapping in and adjacent to the Davis Creek subbasin of the Buffalo River watershed have revealed the geologic framework of this transition between the upper and lower karst aquifers.

Seventeen new dye injection traces conducted by National Park Service in 2001-2003 indicate that the recharge area for Mitch Hill Spring is twice that previously known. Springs in the upper part of the Davis Creek subbasin locally draw interbasin recharge from the adjacent Crooked Creek watershed to the north. Importantly, a losing section in the middle reach of Davis Creek has been documented by a dye trace to contribute to Mitch Hill Spring, connecting it to stream flow from the upper part of the Davis Creek subbasin.

Integration of geologic mapping with the dye tracer results highlights the stratigraphic and structural features that influence ground-water flow. In general, within the erosional relief of the Buffalo River watershed, structural lows localize the largest springs in the perched upper limestone aquifer of the Mississippian Boone Formation whereas structural highs allow recharge and discharge of the lower karst aquifer represented by the lower part of the Ordovician Everton Formation.

Most springs in the upper aquifer discharge near the base of the Mississippian Boone Formation, particularly its basal St. Joe Limestone Member. Local shaley facies in the St. Joe Limestone Member in this area help concentrate the springs at this stratigraphic horizon. As found in a previous study farther west, structural lows formed by faults and folds in the Boone Formation localize the largest springs, including the discharge with known interbasin recharge.

Development of the karst aquifer in the lower part of the Ordovician Everton Formation was facilitated by a change to carbonate-rich facies from sand-rich facies of the formation farther west. The losing reach of Davis Creek coincides with outcrop of lower Everton Formation brought to the surface by uplift along an anticline and monocline. Likewise, Mitch Hill Spring is localized in a dolostone interval near the base of the Everton Formation just above its contact with argillaceous dolostone of the Ordovician Powell Dolomite, a unit of lower karstic permeability. Both formations are exposed where the Buffalo River has eroded into the uplifted side of the northwest-trending Cane Branch monocline. Collapse breccia is widely preserved in sandstone layers just above the dolostone horizon of Mitch Hill Spring, providing further evidence of a major karst network. The west-trending Mill Creek graben intervenes between outcrops of lower Everton Formation at the losing reach of Davis Creek and at Mitch Hill Spring. A ground-water path across this graben probably utilizes down-dropped limestone of the Boone Formation to link flanking zones of lower Everton Formation.